

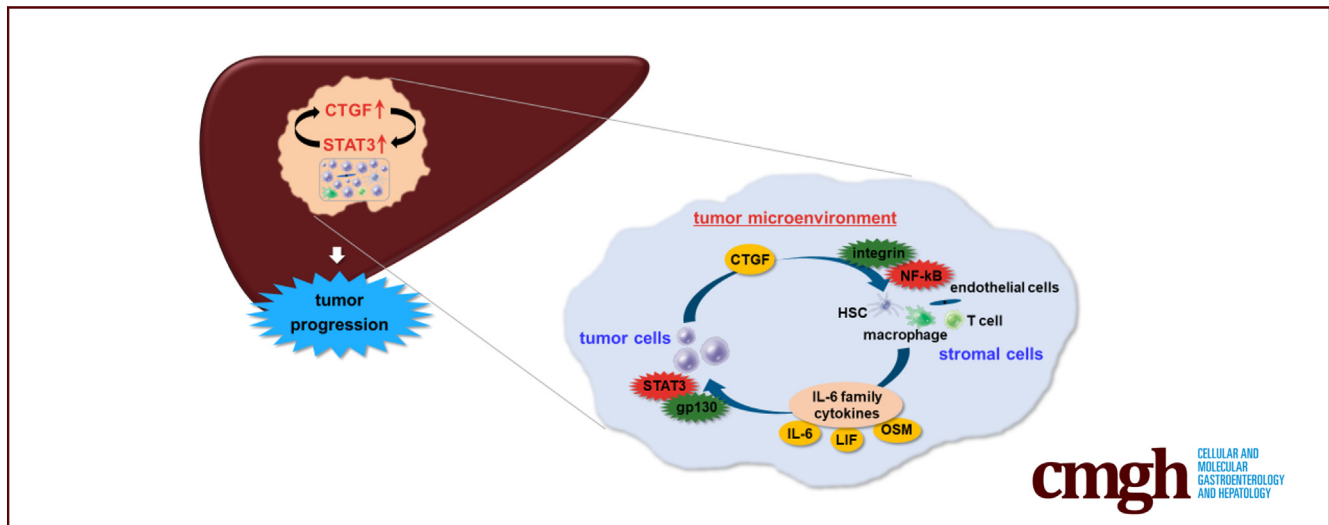
ORIGINAL RESEARCH

STAT3 is Activated by CTGF-mediated Tumor-stroma Cross Talk to Promote HCC Progression



Yuki Makino,¹ Hayato Hikita,¹ Seiya Kato,¹ Masaya Sugiyama,² Minoru Shigekawa,¹ Tatsuya Sakamoto,¹ Yoichi Sasaki,¹ Kazuhiro Murai,¹ Sadatsugu Sakane,¹ Takahiro Kodama,¹ Ryotaro Sakamori,¹ Shogo Kobayashi,³ Hidetoshi Eguchi,³ Nobuyuki Takemura,⁴ Norihiro Kokudo,⁴ Hideki Yokoi,⁵ Masashi Mukoyama,^{5,6} Tomohide Tatsumi,¹ and Tetsuo Takehara¹

¹Department of Gastroenterology and Hepatology, Osaka University Graduate School of Medicine, Osaka, Japan; ²Genome Medical Sciences Project, National Center for Global Health and Medicine, Ichikawa, Japan; ³Department of Gastroenterological Surgery, Osaka University Graduate School of Medicine, Osaka, Japan; ⁴Department of Surgery, National Center for Global Health and Medicine, Tokyo, Japan; ⁵Department of Nephrology, Kyoto University Graduate School of Medicine, Kyoto, Japan; and ⁶Department of Nephrology, Kumamoto University Graduate School of Medical Sciences, Kumamoto, Japan



SUMMARY

Signal transducer and activator of transcription 3 and connective tissue growth factor mutually activated each other via interleukin-6 family cytokine-mediated tumor-stroma crosstalk. This positive feedback loop is a novel molecular and cellular mechanism of hepatocellular carcinoma progression and provides the rationale for therapeutic targets against hepatocellular carcinoma.

BACKGROUND & AIMS: Signal transducer and activator of transcription 3 (STAT3) is known as a pro-oncogenic transcription factor. Regarding liver carcinogenesis, however, it remains controversial whether activated STAT3 is pro- or anti-tumorigenic. This study aimed to clarify the significance and mechanism of STAT3 activation in hepatocellular carcinoma (HCC).

METHODS: Hepatocyte-specific Kras-mutant mice (Alb-Cre Kras^{LSL-G12D/+}; Kras^{G12D} mice) were used as a liver cancer

model. Cell lines of hepatoma and stromal cells including stellate cells, macrophages, T cells, and endothelial cells were used for culture. Surgically resected 12 HCCs were used for human analysis.

RESULTS: Tumors in Kras^{G12D} mice showed up-regulation of phosphorylated STAT3 (p-STAT3), together with interleukin (IL)-6 family cytokines, STAT3 target genes, and connective tissue growth factor (CTGF). Hepatocyte-specific STAT3 knockout (Alb-Cre Kras^{LSL-G12D/+} STAT3^{fl/fl}) downregulated p-STAT3 and CTGF and suppressed tumor progression. In coculture with stromal cells, proliferation, and expression of p-STAT3 and CTGF, were enhanced in hepatoma cells via gp130/STAT3 signaling. Meanwhile, hepatoma cells produced CTGF to stimulate integrin/nuclear factor kappa B signaling and up-regulate IL-6 family cytokines from stromal cells, which could in turn activate gp130/STAT3 signaling in hepatoma cells. In Kras^{G12D} mice, hepatocyte-specific CTGF knockout (Alb-Cre Kras^{LSL-G12D/+} CTGF^{fl/fl}) downregulated p-STAT3, CTGF, and IL-6 family cytokines, and suppressed tumor progression. In human HCC, single cell RNA sequence showed CTGF and IL-6

family cytokine expression in tumor cells and stromal cells, respectively. CTGF expression was positively correlated with that of IL-6 family cytokines and STAT3 target genes in The Cancer Genome Atlas.

CONCLUSIONS: STAT3 is activated by CTGF-mediated tumor-stroma crosstalk to promote HCC progression. STAT3-CTGF positive feedback loop could be a therapeutic target. (*Cell Mol Gastroenterol Hepatol* 2023;15:99–119; <https://doi.org/10.1016/j.jcmgh.2022.09.006>)

Keywords: IL-6 Family Cytokines; Intercellular Interactions; Liver Cancer; Tumor Microenvironment.

Signal transducer and activator of transcription 3 (STAT3) is a cytoplasmic transcription factor that mediates cellular responses to various cytokines or growth factors, such as interleukin (IL)-6.¹ When these extracellular ligands bind to a ligand-specific receptor coupled with the common receptor gp130, gp130 forms a dimer with the ligand-specific receptor. Formation of this receptor complex activates Janus kinase, which activates STAT3 through its phosphorylation. Phosphorylated STAT3 (p-STAT3) dimerizes and moves into the nucleus to enhance the transcription of target genes.² Aberrant activation of STAT3 has been reported in various cancer types and is thought to be involved in oncogenesis.^{2,3} As an oncogene, activated STAT3 enhances multiple cellular processes, including proliferation, survival, antiapoptotic processes, invasion, metastasis, angiogenesis, and immune escape.^{2,3} These actions are mediated by the upregulated expression of its target genes, such as the cell cycle regulators, Cyclin D and c-Myc, and the antiapoptotic proteins, Bcl-2, Bcl-xL, and Mcl1.⁴ STAT3 is considered a key regulator of the proliferation and survival of cancer cells.

Hepatocellular carcinoma (HCC) is the fourth leading cause of cancer-related mortality worldwide.^{5,6} Surgical resection, locoregional ablation, transarterial chemoembolization, and/or systemic drug therapy are performed for the treatment of HCC, depending on the tumor stage and liver function.^{5,6} Although several molecular targeted therapies and immunotherapies have been recently developed, treatment outcomes are still not satisfactory, with a 5-year survival rate of only approximately 30%.⁷ Therefore, novel therapeutic targets have been sought to improve prognosis, and STAT3 might be a candidate. In tumorous tissues, STAT3 is constitutively activated in approximately 60% of HCC cases.^{4,8} Clinically, activation of STAT3 is correlated with poor prognosis and advanced tumor characteristics such as larger tumor size, vascular invasion, and advanced disease stage.^{4,9} As with other malignant tumors, the oncogenic roles of STAT3 have been studied in HCC and shown to be involved in cell proliferation, antiapoptotic processes, migration, invasion, angiogenesis, stemness, and immune suppression.^{4,10} However, almost all of the findings were based on *in vitro* experiments, and these processes have not been sufficiently studied with respect to STAT3 *in vivo*. Therefore, several questions regarding the biology of STAT3 in HCC remain unanswered. For example, the

significance of hepatocyte STAT3 in liver carcinogenesis is controversial. To date, the influence of hepatocyte STAT3 deficiency on hepatocarcinogenesis has been analyzed in 3 liver carcinogenesis models. Whereas some reports showed tumor-suppressive results, others demonstrated completely opposite findings (Table 1).^{11–16} In addition, the molecular mechanisms of STAT3 activation in HCC are not clearly understood. Whereas IL-6 and IL-22 have been presumed to be major stimuli to activate STAT3 in HCC cells,¹⁷ their true impact, as well as the involvement of other cytokines, remains unclear. Furthermore, the types of cells that produce these humoral factors in the tumor microenvironment are unknown.


In the present study, we demonstrated that hepatocyte-specific knockout of STAT3 suppressed tumor progression in 2 different liver carcinogenesis models. Connective tissue growth factor (CTGF) produced by tumor cells is critical for the production of IL-6 family cytokines, which can activate STAT3 in hepatoma cells, stromal cells such as hepatic stellate cells (HSCs), macrophages, T cells, and endothelial cells. In tumor cells, the expression of CTGF, whose protein-coding gene has a STAT3-binding site in its enhancer sequence (Table 2), was enhanced by stimulation with IL-6 family cytokines. These findings provide convincing evidence of the tumor-promoting characteristics of STAT3 in HCC and suggests a novel mechanism of STAT3 activation mediated by tumor-stroma interactions.

Results

STAT3 Was Activated in Liver Tumors in *Kras*^{G12D} Mice, and IL-6 Family Cytokine and CTGF Expression Was Upregulated

As previously reported,¹⁸ *Kras*^{G12D} liver carcinogenesis model mice developed multiple liver tumors at 9 months of age (Figure 1, A–B). In tumorous tissues, several stromal cells, including HSCs, macrophages, endothelial cells, and T cells, were evident and expressing alpha smooth muscle actin (α -SMA), F4/80, platelet endothelial cell adhesion molecule-1 (PECAM-1), and CD3, respectively, as determined by immunohistochemistry (Figure 1, C). Western blotting demonstrated upregulation of p-STAT3, p-Smad2,

Abbreviations used in this paper: α -SMA, alpha smooth muscle actin; CLCF1, cardiotrophin-like cytokine factor 1; CTF-1, cardiotrophin-1; CTGF, connective tissue growth factor; DEN, diethylnitrosamine; HCC, hepatocellular carcinoma; HE, hematoxylin and eosin; HSC, hepatic stellate cell; IL, interleukin; JCRB/HSRRB, Japanese Collection of Research Bioresources/Health Science Research Resources Bank; LIF, leukemia inhibitory factor; LSL, lox P-stop-lox P; NF- κ B, nuclear factor kappa B; NOG, NOD/Shi-scid/IL-2R γ (null); OSM, oncostatin M; PCNA, proliferating cell nuclear antigen; PECAM-1, platelet endothelial cell adhesion molecule-1; p-STAT3, phosphorylated STAT3; qRT-PCR, quantitative real-time reverse-transcription PCR; scRNA-seq, single-cell RNA sequencing; shRNA, short hairpin RNA; siRNA, short interfering RNA; STAT3, signal transducer and activator of transcription 3; UMAP, uniform manifold approximation and projection.

 Most current article

© 2022 The Authors. Published by Elsevier Inc. on behalf of the AGA Institute. This is an open access article under the CC BY-NC-ND license (<http://creativecommons.org/licenses/by-nc-nd/4.0/>).

2352-345X

<https://doi.org/10.1016/j.jcmgh.2022.09.006>

Table 1. Previous Studies in Which the Influence of Hepatocyte-specific Knockout of STAT3 on Liver Carcinogenesis Was Analyzed

Year	Authors	Model	Method of knockout	Tumorigenesis	Tumor size	Ref.
2010	He G, et al.	DEN	Alb-Cre STAT3 ^{fl/fl}	Decreased	Decreased	11
2011	Bard-Chapeau EA, et al.	DEN	Alb-Cre STAT3 ^{fl/fl}	Increased	Increased	12
2011	Wang H, et al.	DEN	Alb-Cre STAT3 ^{fl/fl}	Decreased	Decreased	13
2011	Wang H, et al.	CCI4	Alb-Cre STAT3 ^{fl/fl}	Increased	Increased	13
2017	Abe M, et al.	TAA	Alb-Cre STAT3 ^{fl/fl}	Decreased	Decreased	14

CCI4, Carbon tetrachloride; DEN, diethylnitrosamine; Ref, reference; STAT3, signal transducer and activator of transcription 3; TAA, thioacetamide.

p-Smad3, p-Erk, p-Akt, and CTGF expression in tumorous tissues (Figure 1, D). Immunohistochemistry revealed CTGF upregulation in tumors, mainly in hepatoma cells (Figure 1, E). Quantitative real-time reverse-transcription PCR (qRT-PCR) showed that STAT3-target genes (bcl-2, bcl-xl, cyclin d1, cyclin d2, and myc) and IL-6 family cytokines (leukemia inhibitory factor [lif], oncostatin M [osm], il-11, and clcf1) were upregulated in tumorous tissues (Figure 1, F). The expression of ctgf and tgfb1 was also elevated in tumors (Figure 1, F). In tumorous tissues, the mRNA expression levels of STAT3 target genes and IL-6 family cytokines were positively correlated with the expression of CTGF (Figure 1, G). To analyze the expression of STAT3-target genes, IL-6 family cytokines, and CTGF in tumor cells, we performed single-cell RNA sequencing (scRNA-seq) with tumor tissues. Tumor-consisting cells were divided into clusters of tumor cells, HSCs, endothelial cells, macrophages, T cells, and B cells by uniform manifold approximation and projection (UMAP) plotting (Figure 1, H). The related heat map and UMAP plotting suggested that IL-6 family cytokines were produced by stromal cells, especially HSCs and macrophages, whereas tumor cells expressed only a few of these molecules (Figures 1, H–I). The expression of STAT3 target genes was determined in both tumor cells and stromal cells (Figure 1, I). CTGF-positive cells were found in tumor cells, HSCs, macrophages, and endothelial cells (Figure 1, I). Multiple types of cells were observed to express tgfb1, a potent inducer of CTGF (Figure 1, I).

Hepatocyte-specific Deletion of STAT3 Suppressed Tumor Progression in *Kras*^{G12D} mice, and CTGF Expression Was Downregulated

Among several cell types expressing STAT3-target genes according to the scRNA-seq assay, tumor cells were our primary focus. To analyze the significance of STAT3 expression in hepatocytes/hepatoma cells on the development and progression of liver tumors in *Kras*^{G12D} mice, we generated hepatocyte-specific STAT3-deletion *Kras*^{G12D} mice, and their phenotypes were compared among the 5 following groups of 8-month-old mice: (1) *Kras*^{wild} STAT3^{+/-} mice (STAT3^{+/+} *Kras*^{+/+} Alb-Cre); (2) *Kras*^{wild} STAT3^{-/-} mice (STAT3^{fl/fl} *Kras*^{+/+} Alb-Cre); (3) *Kras*^{G12D} STAT3^{+/-} mice (STAT3^{+/+} *Kras*^{LSL-G12D/+} Alb-Cre); (4) *Kras*^{G12D} STAT3^{+/-} mice (STAT3^{fl/fl} *Kras*^{LSL-G12D/+} Alb-Cre); and (5) *Kras*^{G12D} STAT3^{-/-} mice (STAT3^{fl/fl} *Kras*^{LSL-G12D/+} Alb-Cre).

Liver tumors were not observed in the *Kras*^{wild} groups (Figure 2, A–B). Although there was no difference in tumorigenesis rate among the *Kras*^{G12D} groups, maximum tumor diameter, number of tumors, and the liver/body weight ratio were significantly decreased by STAT3 knockout (Figure 2, A–B). The histological appearance of hematoxylin and eosin (HE)-stained liver tumors did not differ between the 3 groups (Figure 2, C). In the immunohistochemistry assay of proliferating cell nuclear antigen (PCNA), the number of PCNA-positive tumor cells was decreased after STAT3 was knocked out (Figure 2, D). Western blotting of tumorous tissues showed downregulation of p-STAT3 and CTGF expression in *Kras*^{G12D} STAT3^{-/-} mice (Figure 2E). qRT-PCR demonstrated that the expression of CTGF and several STAT3 target genes was downregulated in tumors upon STAT3 knockout (Figure 2, F). In addition, the expression of certain IL-6 family cytokines, such as IL-6, LIF, IL-27, and cardiotrophin-like cytokine factor 1 (CLCF1), was downregulated in tumors in *Kras*^{G12D} STAT3^{-/-} mice (Figure 2, F). STAT3 activation in tumor cells was thus shown to promote tumor progression in *Kras*^{G12D} mice.

Hepatocyte-specific STAT3 Knockout Attenuated Tumor Progression in Model Mice With Diethylnitrosamine (DEN)-induced Liver Carcinogenesis, and CTGF Expression Was Downregulated

The significance of hepatocyte/hepatoma STAT3 on the development and progression of liver tumors was analyzed in DEN-induced liver carcinogenesis model mice. We generated hepatocyte-specific STAT3-null mice and administered DEN to them at 2 weeks of age. The phenotypes between the following 3 groups of 9-month-old mice: (1) STAT3^{+/+} mice (STAT3^{+/+} Alb-Cre); (2) STAT3^{+/-} mice (STAT3^{fl/fl} Alb-Cre); and (3) STAT3^{-/-} mice (STAT3^{fl/fl} Alb-Cre). Macroscopic liver tumors developed in 82.4% to 100% of the mice, and the tumorigenesis rate was not significantly different between the 3 groups (Figure 3, A–B). The maximum tumor diameter, tumor number, and liver/body weight ratio were significantly lower in the STAT3^{-/-} mice than in their STAT3^{+/+} littermates (Figure 3, A–B). The histological appearance of liver tumors in HE staining did not differ between the 3 groups (Figure 3, C). Similar to that observed with liver tumors in *Kras*^{G12D} mice,

Table 2. Enhancer Sequence of the Human ctgf Gene With the STAT3-binding Sequence

Sequence
5'-GGGAATTGGTGCCTTATTTTTTTCAGATTTTCTTGATTTTTTCAACTCT TGTGTATAATAAGTATATTACCATTCTGCTCTGTTGTTAAAAATGTCAAAA GAAAGAATTTGGTTTTACTATAAAATTCATAGTCCCTCGAAGTCTCAAA AAAATCTATAGTCAGTCCAAAATAGATGATTTTAATGTTGCTTAAGAGGAA ATAAGCATATTGAAATATATAGAACATATGAAATCTCAGGAAAGAAAA AGTTTCTGTGCATTATCAGGTTAGATTGAGGCTTTATGATCAAAACTCTTT TTGAAGGAGTAAAAGACTATTATTAAGAGAGTGACACAGAGACAGACA GACACATACATGCACACACACCCAGAGAGAGAGAGAATGAGAGAAGA CACCCAAAGACATTCACAGACTCAGAAGTATGTTTTTATTGTGATAGGACCA TCAAATGCCAGGAAACTCAAAGGGAAAGGCTGATACTCCATCCATCAATT CATGCCATGGGATCTGAATTCCTGCACTATTATCAATGACTCAGCAAATGTT TGTGTGTGCCCTGGGCGGTAAGTGGGAAATAGTGGCTTCTATAACTTCAT CCAACCTTGTACTTACCCAGCCCTTTGATTGACAGCAGGCTCCATCCATCGG AGAAAAAGATCTTTGAATTTGTGTGCAAAATGGTTAAGATGCACTAATTTTG ACTTGTAAAGCAAGTATTTATCTAGCAAAATGCTTTTTAGAGAGCATTTCCT CGTGGTAAAATGAGGAATTAACCTAAGCTGGCCACTGAGTCTGTTACCAA GCTATATAAGGTATGTGTGTGTCTACTAGGCATCATTGTACTGGTGG TTTGGTTAAGCTTGTAAAGATGTTCAAGCTGTGGATGATTACATCTTCCT TAAGTTTTTGTGTTTTTCTCCCTAAAAGAAAAAGGTTTTCTGATCAGGT ATCAGACACAGAAAACTGGCAGGACTACAGAAAAGTGGCCAGAG TTGGAGTGTGTTGTACTTAAAGAAGGAATCTTGACATTTTTCAACTTTTGT TGAGACATTTTCTTACCCAGCCCTTTGATTGACAGCAGGCTCCATCCATCGG CGGAAATCAAAGCTCCAGGAAACATGCCGGAGGAATGTGACTCAGAG CAAAGACCCATACGCATGCATACAGGAGCTGTGACAGCTTATAGGAGG AAGTCTGGCCGTATATGGGCATCTGGCAAGTGGAGCTGAGCCGATTTGCTCT ATGGTGGGTCAGGGGAGGTTCTGATGTTTCTAGCGTGCCTCAAATTC TCATGTAATTAATCTACAAAAAATGGTATCCAGAGGCTTTTGTAA ATAGTAATAAATATTCTGAAATCTCAGGGACCTGGTTGGCTGACAT GACCTCTGTTGCTTAAAGTGAAGGTTAAGGAGAGGGCGTACTTGTGG GAGTTCATGCGGGGAAAGATAAACCGCGGATGTTTACTATCTAAATTA CTTCATTACCTTCATGCCCTTTCCCTCCTTATAATTAGTTCCTGACTT CTTAGGATATTTCTAATGCAAGGATTTGTGCAAGGCGAGTCAAGG CCGTTGCATGTGGTTTTGTGTTTGTGCTGTTTCCCTGCTTGTCCA TAGAGTTGGAGGCCAGAGGGTGAAGAAAGGAAGTTTTGTTGTAAGATG ATATCCCTTCAACTACTGTTTGTTCACCTATTTTGTAAATTTGACTCTT TTTTTTTTAAAGTAGTTTACTTAGAATCCTGTGTGCCTCTAGTCACTTT TGTTCACTAAGATAGTGCAGATGAGGATGCTGCTAGTAGGAATGAGC CTGGTGGTCTCTTACACTGCTCCTCGACAGGTTAGAATCTCAAATTCATCAC CGTTTAGCAACCAGGAGTATTTACAGCCCTTGCCTCATCAGGGCTAAAT GTGAAGCATCCCTTGGTGATACTTAAGGTGATTTAAGTGAAGTGGGAAT GAAAAACAGAGGAAATAAGCAATTTCTAAGATGTGTGATTTGGGGACACC CAATCAATAGGTTTAGGAGGAAGAGAAATGGGACTAGCTATCTTATCT CAAATAATAGAAGTAAGTGAAGGATAAATTTTTGAAAGGACTAGTGTGA AATACATGAATGATTTCTTAGGGATCTGCTGCGGGGTGGAAAGGG GTGCAGATTAAAGCCAGACCCATCATTATCCCTGGAATGTGCTCCAC CTTAGCCAAGAGGCTGAGTCCCTTCTCACAACCTCAAACCTCCCTGG AATACCATTAGGTGGAGCTTAGGGACTGGCTAGGAGGTGAAGGTGTGA GCTCCATACCTGCCATTTGCTTGCAGTGACCTCAGGGAAGACACCTAC TCTCTGTAGCCTGAAATTTCCACCTGTTCCACAGTTAATGTGCAGCTC AAGGAGACAATATTATGAAAGCACTTTCAAAAAGGTTATAGATTTTTAA AATTGCCCTTCTCTTCCATTCTCAGTGGCTCTCAAACCTAAGCCCAAC TCAGATTGACTGTAAGGCTGTACAGTGTGATTTTATAACAGTGTCCA GCTCTGCATGGTTTTAGAGTGTAAACACTAGGTGAGAGCTCAGAGAA AATCAAATCCTACCTTATTTATTTATTTTATTAGATTAGATATTACAG GATTGATAGACATTTAAACAAATGAAACTTTTTTCTTTTTGAAATAGGG TCTGGCTCTGCTCCAGGGTGGAAATGTAG-3'

Note: The STAT3-binding sequence is underlined and presented in bold. STAT3, Signal transducer and activator of transcription 3.

immunohistochemistry revealed several stromal cells in DEN-induced liver tumors, including HSCs, macrophages, endothelial cells, and T cells, expressing α -SMA, F4/80, PECAN-1, and CD3, respectively (Figure 3, D). The number of PCNA-positive hepatoma cells was the smallest in the STAT3^{-/-} group (Figure 3, E). According to the Western blot results, the expression of p-STAT3 and CTGF was elevated in the liver tumors compared with nontumor tissues of STAT3^{+/+} mice (Figure 3, F). CTGF expression was up-regulated in tumor tissues compared with adjacent nontumor

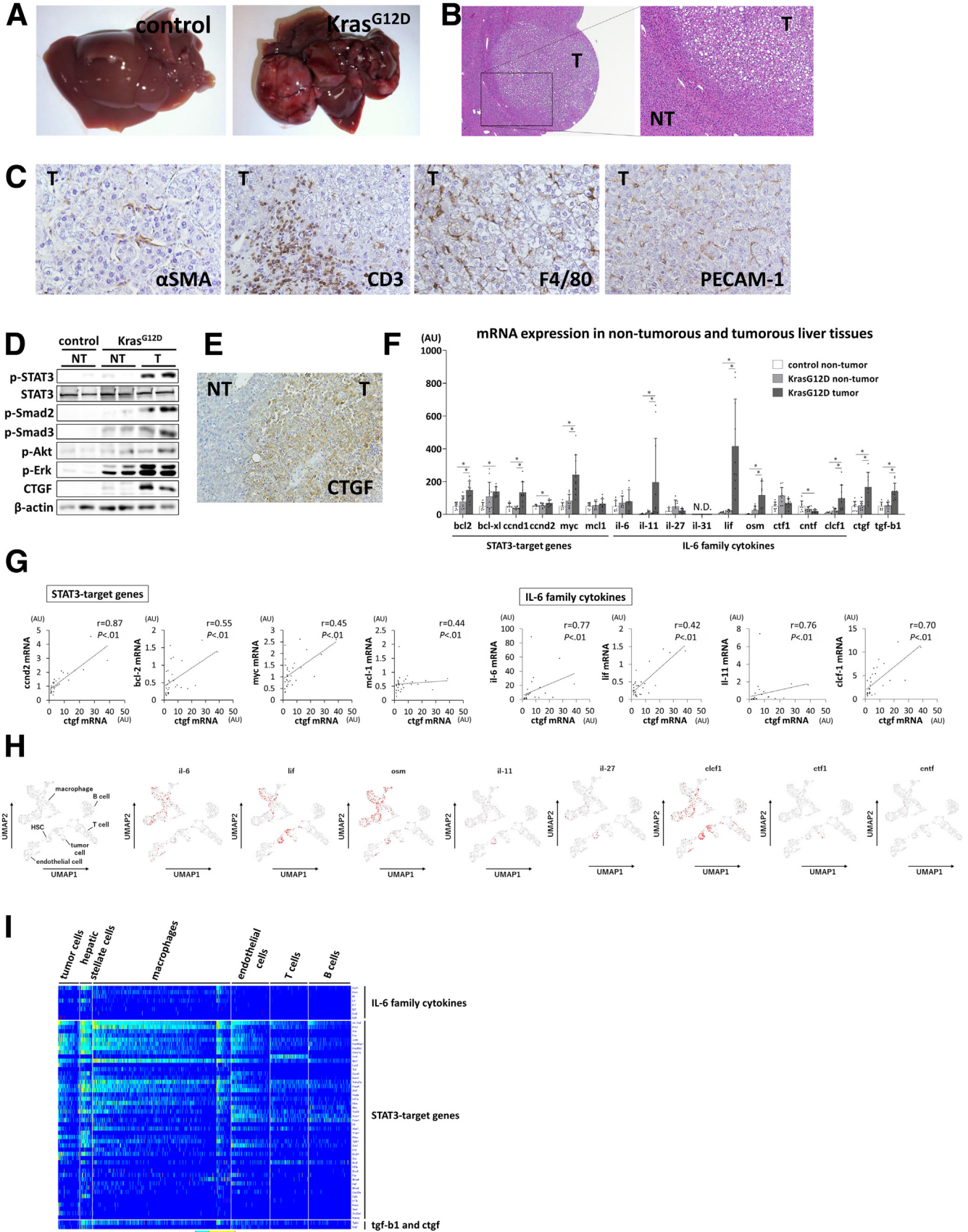
liver tissues (Figure 3, G). In comparison to that in STAT3^{+/-} mice, p-STAT3 and CTGF expression was downregulated in the tumor tissues of STAT3^{-/-} mice (Figure 3, F). qRT-PCR demonstrated that the expression of STAT3-target genes (bcl-2, bcl-xl, ccnd1, ccnd2, and myc), IL-6 family cytokines (lif, osm, and clcf1), and ctgf was upregulated in tumor tissues compared with nontumor tissues in STAT3^{+/+} mice (Figure 3, H), and the gene expression patterns were similar to those of Kras^{G12D} tumors. In liver tumors of STAT3^{-/-} mice, the expression of several STAT3-target genes (bcl-2, ccnd2, and myc), IL-6 family cytokines (osm and clcf1), and ctgf was downregulated compared with that in STAT3^{+/+} mice (Figure 3, H). Hepatocyte-specific STAT3 knockout gave rise to similar phenotypes and molecular profiles between DEN- and Kras-induced liver carcinogenesis models.

Expression of p-STAT3 and CTGF Expression and the Cell Proliferation Rate in Hepatoma Cells Were Increased by Stromal Cells Via gp130/STAT3 Signaling

In vitro, we first analyzed the significance of STAT3 on the proliferation of hepatoma cells. Short interfering RNA (siRNA)-mediated knockdown of STAT3 did not affect the proliferation of HepG2 or Alex cells (Figure 4, A). STAT3 knockdown did not decrease but slightly increased CTGF expression in HepG2 cells in monoculture but did not affect CTGF expression in Alex cells (Figure 4, B). We next focused on stromal cells to analyze the mechanisms and significance of STAT3 activation in tumor cells. We cocultured hepatoma cells and stromal cells and then performed Transwell assays to examine the proliferation and expression of p-STAT3 and CTGF in hepatoma cells. Coculture with LX-2, THP-1, MTA, or TMNK-1 cells, which are HSCs, macrophages, T cells, or liver sinusoidal endothelial cells, respectively, increased p-STAT3 and CTGF expression in HepG2 cells, which showed a higher proliferation rate (Figure 4, C–D). Similar expression changes were observed in Alex cells (Figure 4, C). Proliferation of Alex cells was increased by the coculture with THP-1 cells (Figure 4, D). In contrast to the slight increase in CTGF expression under monoculture, STAT3 knockdown down-regulated CTGF and p-STAT3, in HepG2 cells under coculture with stromal cells (Figure 4, E). STAT3 knockdown also decreased CTGF and p-STAT3 expression in Alex cells under coculture (Figure 4, E). Additionally, siRNA-mediated knockdown of gp130 attenuated p-STAT3 and CTGF expression in HepG2 cells under both monoculture and coculture conditions (Figure 4, F). Alex cells showed similar results (Figure 4, F). The viability of HepG2 and Alex cells was decreased by knockdown of either STAT3 or gp130 under coculture with stromal cells, but it was not affected under monoculture (Figure 4, G).

IL-6 Family Cytokines Upregulated p-STAT3 and CTGF Expression and Increased the Hepatoma Cell Proliferation Rate Via gp130/STAT3 Signaling

As ligands of gp130, we focused on IL-6 family cytokines as factors to increase proliferation and up-regulate CTGF in



HepG2 cells co-cultured with stromal cells. IL-6, LIF, and OSM, representative 3 IL-6 family molecules, were specifically secreted by stromal cell lines in monoculture (Figure 5, A). Exposure to IL-6, LIF, or OSM increased p-STAT3 expression in HepG2 and Alex cells in monoculture (Figure 5, B). Treatment with IL-6, LIF, or OSM also upregulated CTGF expression in HepG2 and Alex cells (Figure 5, C). IL-6, LIF, and OSM facilitated the proliferation of HepG2 and Alex cells (Figure 5, D). When gp130 was knocked down by siRNA, up-regulation of CTGF after the treatment with IL-6, LIF, or OSM was attenuated both in HepG2 and Alex cells (Figure 5, E). Similarly, siRNA-mediated knockdown of STAT3 decreased CTGF expression upon exposure to IL-6, LIF, or OSM (Figure 5, E). The increase in hepatoma cell proliferation induced by treatment with IL-6, LIF, or OSM was abrogated by siRNA-mediated knockdown of either gp130 or STAT3 in both HepG2 and Alex cells (Figure 5, F). In summary, IL-6, LIF, and OSM increased CTGF expression and the proliferation of hepatoma cells in a gp130/STAT3 signaling-dependent manner.

Exposure to HSCs Increased the Growth of Xenograft Tumors Via gp130/STAT3 Signaling

To analyze the influence of stromal cells on cell proliferation and CTGF expression in xenograft models, HepG2 cells were transfected with gp130 short hairpin RNA (shRNA) (HepG2-gh130sh cells), STAT3 shRNA (HepG2-STAT3sh cells) or control shRNA (HepG2-control sh cells) to generate stable knockdown cell lines (Figure 6, A). Neither gp130 shRNA nor STAT3 shRNA affected the proliferation of HepG2 cells in vitro (Figure 6, A). Among the 5 stromal cell lines assessed, LX-2 cells have often been utilized for coinoculation experiments with hepatoma cells to study tumor-stroma interactions in HCC.¹⁸⁻²⁰ Therefore, we generated subcutaneous tumors composed of HepG2 cells alone or HepG2 cells mixed with LX-2 cells. Similar to reports of previous studies,¹⁸⁻²⁰ when HepG2-control sh cells were coinoculated with LX-2 cells, the growth of xenograft tumors was enhanced compared with the effect of HepG2-control sh cells alone (Figure 6, B). However, the growth of xenograft tumors was not increased by the coinoculation of HepG2-gp130sh cells and LX-2 cells (Figure 6, B). Both gp130 and CTGF mRNA expression in the xenograft tumors was decreased by shRNA-mediated gp130 knockdown in HepG2 cells in the presence of LX-2 cells (Figure 6, B).

Immunohistochemistry showed a decrease in p-STAT3 positive tumor cells in xenograft tumors composed of HepG2 cells transfected with gp130 shRNA (Figure 6, B). Similar to the effect of gp130 shRNA, the growth of xenograft tumors composed of HepG2-STAT3sh cells was not enhanced by coinoculation with LX-2 cells (Figure 6, C). Both STAT3 and CTGF mRNA expression was lower in xenograft tumors composed of HepG2-STAT3sh cells and LX-2 cells than in those composed of HepG2-control sh cells and LX-2 cells (Figure 6, C). In immunohistochemistry of xenograft tumors, p-STAT3 positive tumor cells were decreased by STAT3 shRNA in HepG2 cells (Figure 6, C).

CTGF Produced by Hepatoma Cells Upregulated IL-6 Family Cytokines in Stromal Cells, Enhanced p-STAT3 Expression in Hepatoma Cells and Increased the Hepatoma Cell Proliferation Rate

We next analyzed the significance of hepatoma cell CTGF on STAT3 activation and the proliferation of hepatoma cells cocultured with stromal cells. Recombinant CTGF treatment did not change p-STAT3 expression in hepatoma cells (Figure 7, A). In coculture with LX-2, THP-1, MTA, or TMNK-1 cells, HepG2 cells with CTGF knocked down showed downregulation of both CTGF and p-STAT3 expression (Figure 7, B). In addition, knocking down CTGF in HepG2 cells abrogated the increase in the HepG2 proliferation rate induced by coculturing with stromal cells, whereas CTGF knockdown did not affect HepG2 proliferation under monoculture conditions (Figure 7, C). We next analyzed the influence of CTGF knockdown in HepG2 cells on IL-6 family production in stromal cells. HepG2 cells were transfected with CTGF siRNA or control siRNA and subsequently cocultured with stromal cell lines. Coculture with HepG2 cells transfected with control siRNA upregulated multiple IL-6 family cytokines in stromal cell lines, whereas only LIF, Clcf1, and IL-11 were downregulated in THP-1 cells (Figure 7, D). Under coculture conditions, CTGF knockdown in the HepG2 cells led to decreased expression of most IL-6 family cytokines in the stromal cell lines (Figure 7, D). In culture supernatant, HepG2 cells hardly secreted IL-6 under monoculture (Figure 7, E). CTGF knockdown in HepG2 cells decreased the IL-6 concentration in supernatant under coculture with MTA and TMNK-1 cells (Figure 7, E).

Figure 1. (See previous page). Hepatocyte-specific *Kras*-mutant mice developed liver tumors with STAT3 activation and upregulation of CTGF and IL-6 family cytokine expression in hepatoma cells and stromal cells, respectively. *Kras*^{G12D} mice and their littermate Alb-Cre transgenic control mice were sacrificed at 7 to 12 months of age and their phenotypes were compared (A-G). A, Representative images of the livers at 9 months of age. B, HE staining of a liver tumor (left; $\times 40$, right; $\times 100$). C, Immunohistochemistry results showing α -SMA, CD3, F4/80, and PECAM-1 in liver tumors in *Kras*^{G12D} mice ($400\times$). D, Western blot showing liver tissue proteins. E, Immunohistochemistry results showing CTGF in the liver of *Kras*^{G12D} mice ($200\times$). F, mRNA expression of STAT3 target genes, IL-6 family cytokines, *ctgf*, and *tgf-b1* in liver tissues ($n = 7-12$). G, Correlation of mRNA expression between CTGF and STAT3-target molecules and IL-6 family cytokines ($n = 20$). Liver tumors were collected from a 12-month-old mouse harboring the *Kras*^{G12D/+} allele and subjected to single-cell RNA sequencing (scRNA-seq) (H-I). In total, 1303 cells from 2 tumors were analyzed. H, UMAP plots of IL-6 family cytokines. I, Heat map of IL-6 family cytokines, STAT3-target genes, *tgf-b1*, and *ctgf* according to the cell types. For immunohistochemistry, a representative image of each molecule from 6 samples was presented. NT, Nontumor tissues; T, tumor tissues. * $P < .05$.

CTGF Upregulated IL-6 Family Cytokine Expression Via Integrin-mediated Nuclear Factor Kappa B (NF- κ B) Activation in Stromal Cells

We subsequently examined the influence of CTGF treatment on IL-6 family cytokine production in stromal cells. After treatment with recombinant CTGF protein, the expression of several IL-6 family cytokines, except Cardiotrophin-1 (CTF-1), was upregulated, and simultaneously, NF- κ B was activated in LX-2, THP-1, MTA, and TMNK-1 cells (Figure 8, A). We next blocked integrins, cell-surface receptors of CTGF, with the RGDS peptide, an inhibitor of integrin receptor function. When LX-2, THP-1, MTA, and TMNK-1 cells were pretreated with the RGDS peptide, activation of NF- κ B was not observed even after recombinant CTGF treatment (Figure 8, B). Furthermore, CTGF-mediated upregulation was abrogated by RGDS pretreatment of most IL-6 family cytokine-expressing stromal cells (Figure 8, B). To analyze the significance of NF- κ B activation on IL-6 family cytokine production, cells were pretreated with SN-50, an inhibitor of nuclear translocation of activated NF- κ B. When LX-2, THP-1, MTA, and TMNK-1 cells were pretreated with SN-50 before recombinant CTGF treatment, the upregulation of most IL-6 family cytokines was attenuated (Figure 8, C).

Hepatocyte-specific Deletion of CTGF Led to Downregulated IL-6 Family Cytokine Expression in Liver Tumors, Suppressed STAT3 Activation and Inhibited Tumor Progression in *Kras*^{G12D} Mice

The roles of hepatocyte CTGF were subsequently analyzed in *Kras*^{G12D} mice. Our previous report demonstrated that hepatocyte-specific CTGF knockout downregulated p-STAT3 expression and suppressed the progression of liver tumors in *Kras*^{G12D} mice.¹⁸ In the present study, we analyzed the influence of hepatocyte-specific CTGF knockout on the expression of STAT3 target genes and IL-6 family cytokines in liver tumors. Hepatocyte-specific CTGF-deleted *Kras*^{G12D} mice were generated, and the phenotypes of the following 3 groups were compared at 8 months of age: (1) *Kras*^{G12D} CTGF^{+/+} mice (CTGF^{+/+} *Kras*^{LSL-G12D/+} Alb-Cre); (2) *Kras*^{G12D} CTGF^{+/-} mice (CTGF^{fl/+} *Kras*^{LSL-G12D/+} Alb-Cre); and (3) *Kras*^{G12D} CTGF^{-/-} mice (CTGF^{fl/fl} *Kras*^{LSL-G12D/+} Alb-Cre). As we previously reported,¹⁸ CTGF deletion in hepatocytes suppressed tumor progression (Figure 9, A) and downregulated p-STAT3 expression (Figure 9, B). qRT-PCR demonstrated that CTGF expression in liver tumors was significantly decreased by hepatocyte-specific CTGF deletion in *Kras*^{G12D} mice (Figure 9, C). In addition to that of CTGF, the expression of multiple STAT3-target genes and IL-6 family cytokines was downregulated in liver tumors in *Kras*^{G12D} CTGF^{-/-} mice (Figure 9, C). These findings suggested that CTGF produced by tumor cells enhanced IL-6 family cytokine production and STAT3 activation in liver tumors, leading to tumor progression in *Kras*^{G12D} mice.

The Expression of CTGF Was Positively Correlated With That of STAT3 Target Genes and IL-6 Family Cytokines in Human HCC

The relationship of CTGF with STAT3 activation and IL-6 family cytokine production was examined in human HCC samples. According to the immunohistochemistry assay, CTGF was positively expressed in tumor cells (Figure 10, A). The immunohistochemistry results also demonstrated the presence of α -SMA-positive HSCs, CD3-positive T cells, CD68-positive macrophages, and PECAM-1-positive endothelial cells (Figure 10, A). scRNA-seq of surgically resected HCC tissues demonstrated the presence of CTGF-positive cells in clusters of tumor cells, HSCs, and endothelial cells (Figure 10, B). The expression of IL-6 family cytokines was found in clusters of stromal cells, such as HSCs, macrophages, endothelial cells, and T cells (Figure 10, B). We next analyzed the relationship of CTGF with IL-6 family cytokines and STAT3 target genes using The Cancer Genome Atlas database. CTGF gene expression was positively correlated with 6 (IL-6, LIF, OSM, CLCF-1, IL-11, and CTF-1) of 9 IL-6 family cytokines (Figure 10, C). CTGF mRNA expression was also positively correlated with that of 27 STAT3 target genes (Figure 10, C).

Discussion

In the present study, we demonstrated that activated STAT3 accelerated the progression of liver cancer, as evidenced by the results of hepatocyte-specific STAT3-knockout mice (Figures 2 and 3). Additionally, this tumor-promoting effect was shown to be due to tumor-stromal cross talk mediated by CTGF and IL-6 family cytokines. In hepatoma cells grown in monoculture, knockdown of STAT3 in vitro did not decrease the proliferation rate of the hepatoma cells or the expression of CTGF (Figure 4). These results suggested that STAT3 in hepatoma cells might not be as significantly influential as to show tumor-promoting functions in the absence of external stimuli. Meanwhile, in the presence of stromal cells, hepatoma cell STAT3 was activated and promoted hepatoma cell proliferation and CTGF expression both in vitro and in xenografts (Figures 4 and 6). These findings indicated that STAT3 drives function especially in the settings of tumor microenvironment. Previous reports regarding STAT3 in HCC have focused solely on hepatoma cells, and reports on its significance in the tumor microenvironment have been rare. By investigating the roles of STAT3 in tumor-stromal interactions, our findings show a novel role for STAT3 in HCC.

With regard to the influence of STAT3 knockout on liver carcinogenesis, the discrepancies between previous studies (Table 1) might be partly explained by the influence of background liver inflammation. Due to the hepatoprotective roles of hepatocyte STAT3,^{21,22} hepatocyte-specific STAT3 knockout may augment liver injury and fibrosis, which can accelerate tumorigenesis. Therefore, even if knocking out hepatoma STAT3 suppresses tumor growth, tumor incidence may be accelerated by STAT3 deletion in hepatocytes in HCC models with severe liver injury, such as CCl4 models.¹³ Because background liver injury or fibrosis is

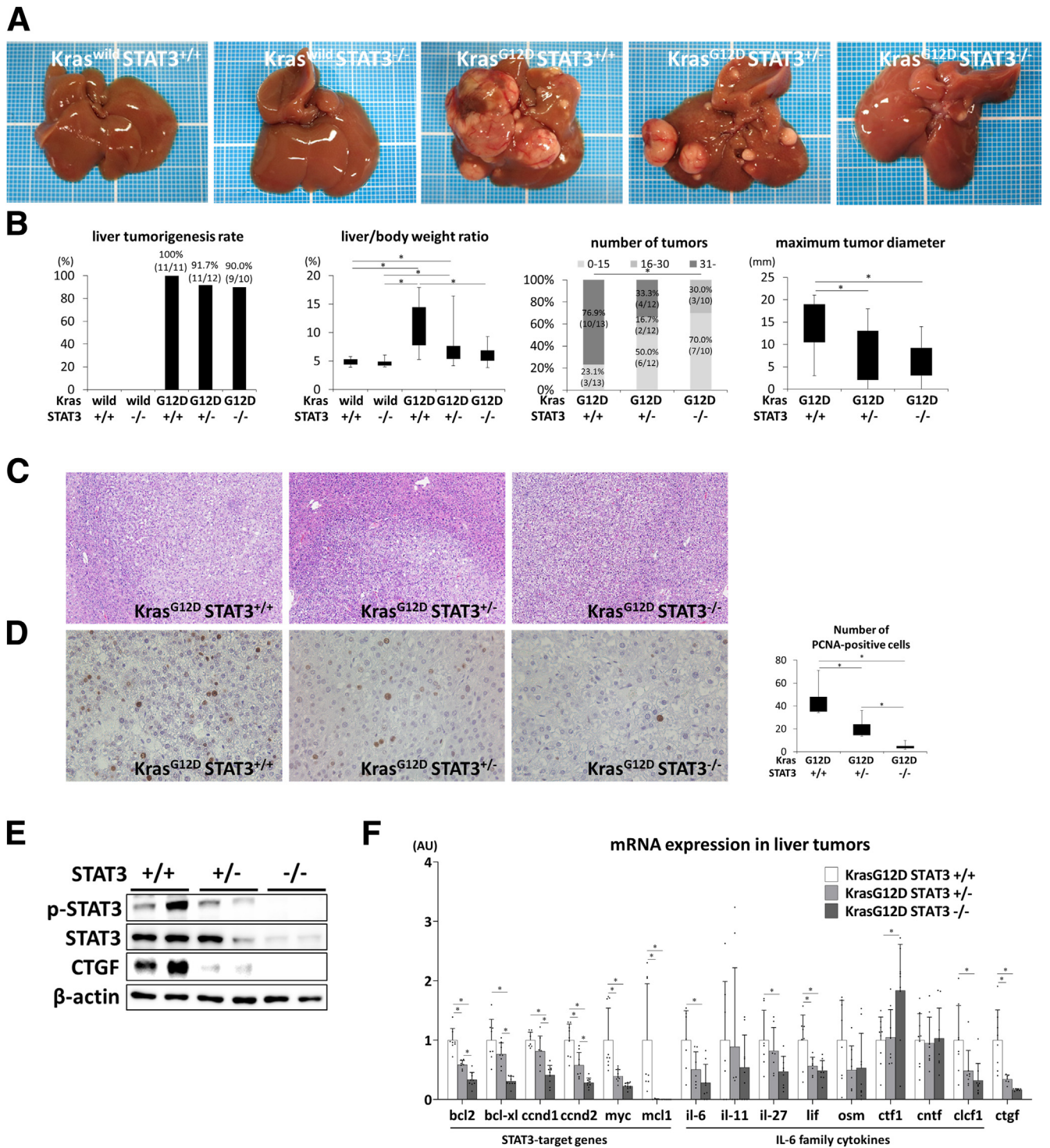
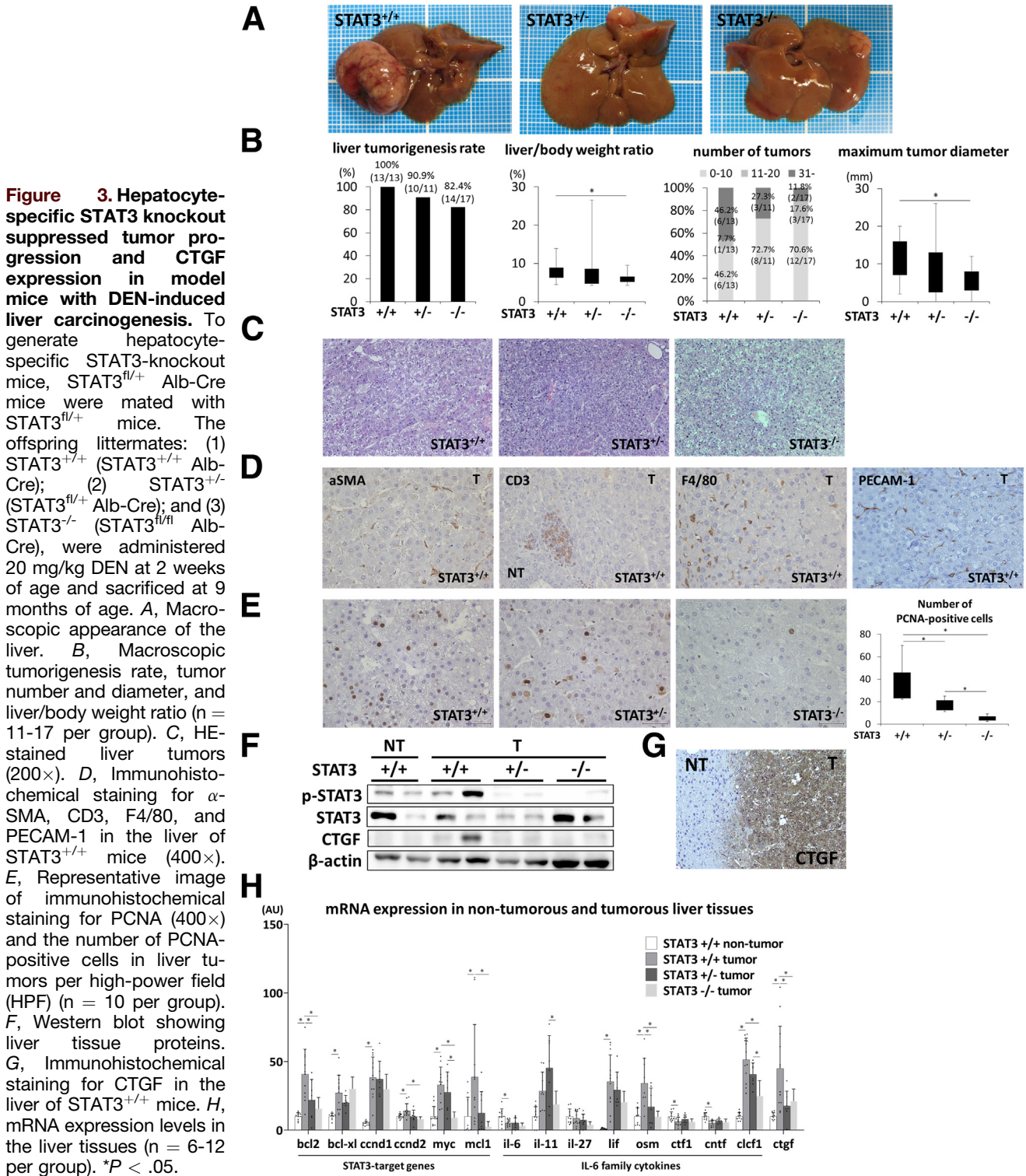
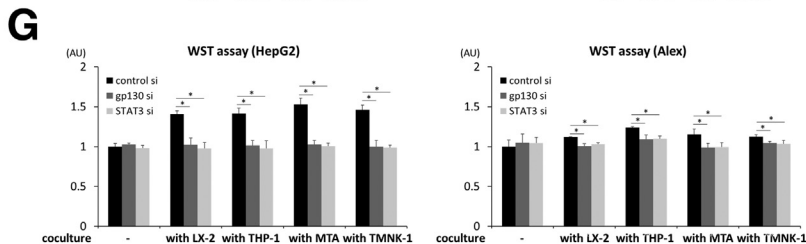
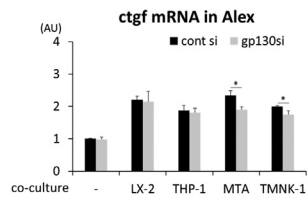
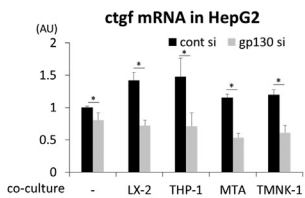
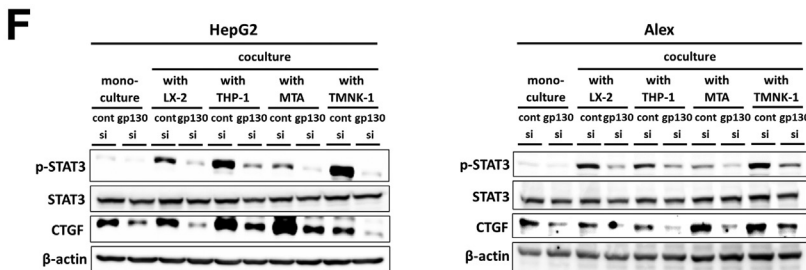
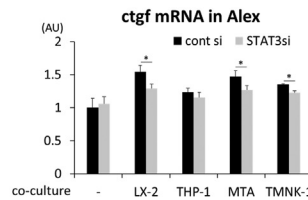
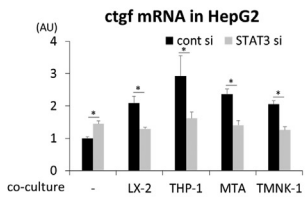
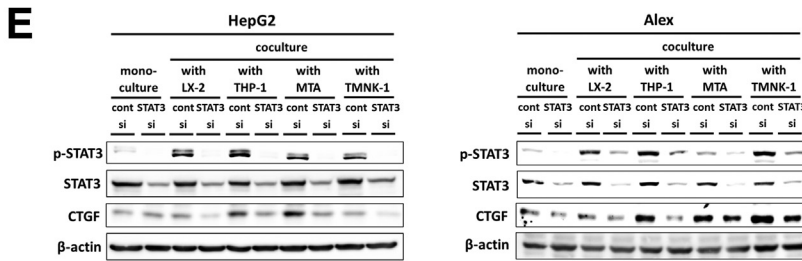
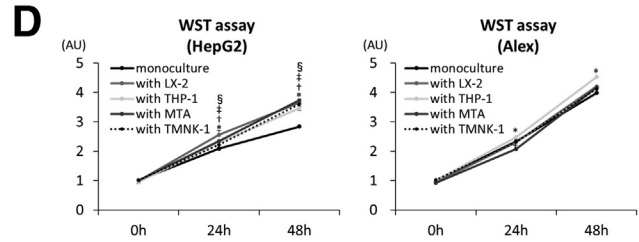
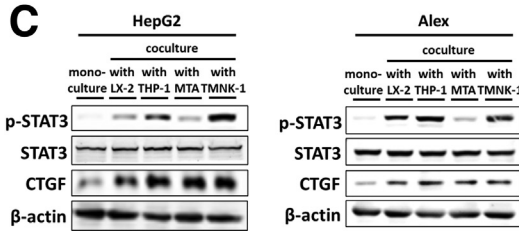
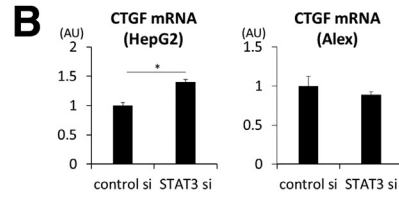
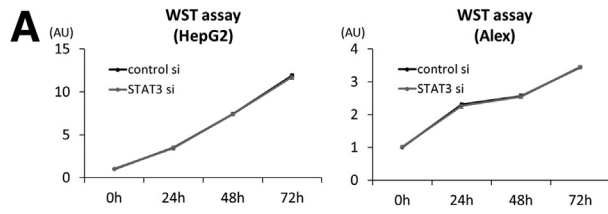


Figure 2. Hepatocyte-specific STAT3 knockout suppressed tumor progression and CTGF expression in liver tumors of *Kras*^{G12D} mice. *Kras*^{G12D} mice and STAT3-floxed mice were mated to generate hepatocyte-specific STAT3-knockout *Kras*^{G12D} mice. After mating STAT3^{fl/+} *Kras*^{+/+} Alb-Cre mice and STAT3^{fl/+} *Kras*^{LSL-G12D/+} mice, the offspring: (1) *Kras*^{wild} STAT3^{+/+} (STAT3^{+/+} *Kras*^{+/+} Alb-Cre); (2) *Kras*^{wild} STAT3^{-/-} (STAT3^{fl/fl} *Kras*^{+/+} Alb-Cre); (3) *Kras*^{G12D} STAT3^{+/+} (STAT3^{+/+} *Kras*^{LSL-G12D/+} Alb-Cre); (4) *Kras*^{G12D} STAT3^{+/-} (STAT3^{fl/+} *Kras*^{LSL-G12D/+} Alb-Cre); and (5) *Kras*^{G12D} STAT3^{-/-} (STAT3^{fl/fl} *Kras*^{LSL-G12D/+} Alb-Cre) littermates were sacrificed at 8 months of age. **A**, Representative images of the livers. **B**, Macroscopic liver tumorigenesis rate, liver/body weight ratio, tumor number, and maximum tumor diameter (n = 8-12 per group). **C**, Representative images of HE staining of liver tumors. **D**, Representative images of immunohistochemical staining for PCNA (400×) and the number of PCNA-positive cells in liver tumors per each high-power field (HPF) (n = 10 per group). **E**, Western blot showing liver tumor proteins. **F**, Gene expression of STAT3-target genes, IL-6 family cytokines, and CTGF in liver tumors (n = 5-9). *P < .05.



absent in our Kras-mutant model,¹⁸ the inflammation-fibrosis-carcinogenesis sequence in human HCC was not recapitulated in our model mice. In DEN models, persistent liver inflammation is usually not found, although transient liver injury is observed shortly after DEN administration.¹¹⁻

¹³ Taking advantage of this outcome, we can specifically focus on the tumor microenvironment in these models, excluding the influence of background liver inflammation or fibrosis. In tumor tissues of both models, several stromal cells were found to be in close proximity to tumor cells



(Figure 1, C and Figure 3, D), similar to their localization in the human HCC microenvironment (Figure 10, A). Using these models, we clearly demonstrated that hepatocyte-specific STAT3 knockout attenuated the proliferation of tumor cells and inhibited CTGF expression, leading to the suppression of tumor progression. Our findings provide substantial evidence that activated STAT3 in hepatoma cells accelerates tumor progression in vivo.

As activators of STAT3, several IL-6 family cytokines were upregulated in HCC in our study. Additionally, our scRNA-seq analysis revealed the expression profile of IL-6 family cytokines in the tumor microenvironment. IL-6 family cytokines consist of 9 molecules, IL-6, IL-11, IL-27, IL-31, OSM, LIF, CLCF1, ciliary neurotrophic factor, and CTF-1.^{23,24} Activation of the STAT3 signaling pathway is the hallmark of IL-6 family function. Distortion of these cytokine activities can promote cancer initiation and progression.^{23,24} Among these cytokines, IL-6 has been the most extensively studied and has been implicated in hepatocarcinogenesis²⁵; however, little is known about the functions of other molecules in HCC.²³ Expression of IL-6 cytokine family molecules was noted in stromal cells such as HSCs, macrophages, T cells, and endothelial cells (Figure 1 and Figure 10). Although HSCs and macrophages are known to produce multiple humoral factors that modulate tumor biology, endothelial cells and T cells have not attracted attention as cytokine producers in the HCC microenvironment.²⁶⁻²⁸ Our Transwell coculture experiments demonstrated that all of the stromal cell types examined increased p-STAT3 and CTGF expression and the proliferation of hepatoma cells without direct contact, probably via some humoral factors. IL-6, LIF, and OSM were shown to upregulate p-STAT3 and CTGF expression and facilitate the proliferation of hepatoma cells via gp130/STAT3 signaling (Figure 5). These findings suggested that IL-6 family cytokines were powerful candidates that mediated the increase in p-STAT3 and CTGF expression and the proliferation of hepatoma cells cocultured with stromal cells. In addition to the effect on tumor cells, the conspicuous expression of STAT3-target genes in stromal cells suggests the possibility that IL-6 family cytokines also act on stromal cells, via either or both an autocrine manner or stroma-stroma interaction. The influence of IL-6 family cytokines on stromal cells in HCC should also be of interest. In the next step, the significance of each molecule should be validated in vivo as a novel mediator of the tumor microenvironment in HCC.

CTGF, also known as CCN2, is a secreted matricellular protein associated with the fibrosis of several organs, including the liver.²⁹ Recently, CTGF has attracted attention as a therapeutic target in several cancer types.^{30,31} Clinical trials of anti-CTGF therapy have been initiated.³² Meanwhile, because CTGF has numerous and diverse mechanisms of action, affecting both cellular and matrix components of tumors, how CTGF exerts its function in each cancer type, including HCC, has not been determined.³⁰ In our previous study, we reported that CTGF was overexpressed in hepatoma cells and promoted HCC progression, possibly by increasing IL-6 production in HSCs, which activates STAT3 in hepatoma cells.¹⁸ However, it remains unclear whether the target of CTGF is only IL-6 in HSCs. In addition, the mechanism of CTGF-induced IL-6 upregulation in HSCs has not been clarified. In the present study, we revealed that CTGF induced the production of several IL-6 family cytokines in multiple stromal cells via integrin/NF- κ B signaling and that this effect was not limited to IL-6 in HSCs. Because IL-6 family cytokines mediate CTGF upregulation in hepatoma cells, hepatoma STAT3 and CTGF form a positive feedback loop to upregulate each other via IL-6 family cytokines produced by stromal cells. The discovery of this feedback mechanism leads to the question, what triggers this positive feedback loop? In addition to revealing the upregulation of p-STAT3, we showed the activation of TGF- β /Smad signaling and Ras signaling in liver tumors in our Kras-mutant model (Figures 1, D and F). Both the TGF- β /Smad and Ras/Mek/Erk signaling pathways are frequently activated in HCC and are inducers of CTGF expression,^{9,33,34} suggesting the possibility that upregulation of CTGF might be the trigger of the aforementioned positive feedback loop. With regard to the source of CTGF in HCC microenvironment, scRNA-seq in the present study clearly demonstrated that CTGF was expressed in tumor cells, HSCs and endothelial cells (Figures 1, H; 1, I; and 10, B). Although the significance of CTGF produced by HSCs or endothelial cells has not been addressed, our experiments with hepatocyte-specific CTGF knockout mice indicated that tumor cells were important sources of CTGF for up-regulation of IL-6 family cytokines and tumor progression of liver cancer (Figure 9). Our findings thus suggest a novel action of CTGF produced by tumor cells, as well as the mechanisms of CTGF and p-STAT3 upregulation in HCC.

One limitation of the present study is that we used cell lines, instead of primary stromal cells, for culture

Figure 4. (See previous page). Stromal cells increased p-STAT3 and CTGF expression and cell growth in hepatoma cells. HepG2 or Alex cells were transfected with STAT3 siRNA or control siRNA (A-B). WST-8 assay (A) and CTGF mRNA expression (B) of HepG2 or Alex cells after siRNA transfection. Total RNA was collected 48 hours after siRNA transfection. HepG2 or Alex cells were incubated in monoculture or cocultured with LX-2, THP-1, MTA, and TMNK-1 cells, using Transwell insert system (C-G). THP-1 cells were pretreated with 100 ng/mL phorbol 12-myristate 13-acetate (PMA) for 48 hours to induce macrophage differentiation before coculturing. Total proteins and RNA were collected after 24 hours of incubation (C, E, F). C, Western blot showing protein expression of HepG2 or Alex cells. D, WST-8 assay of HepG2 or Alex cells in coculture at the indicated time points. HepG2 or Alex cells were transfected with STAT3 siRNA, gp130 siRNA, or control siRNA 48 hours before coculturing (E-G). E, Western blot showing protein expression and qPCR showing CTGF mRNA expression in HepG2 or Alex cells transfected with STAT3 siRNA or control siRNA. F, Western blot and CTGF mRNA expression in HepG2 or Alex cells transfected with gp130 siRNA or control siRNA. G, WST-8 assay of HepG2 or Alex cells transfected with STAT3 siRNA, gp130 siRNA, or control siRNA 48 hours after incubation (n = 3-4). *, †, ‡, §P < .05 vs control.

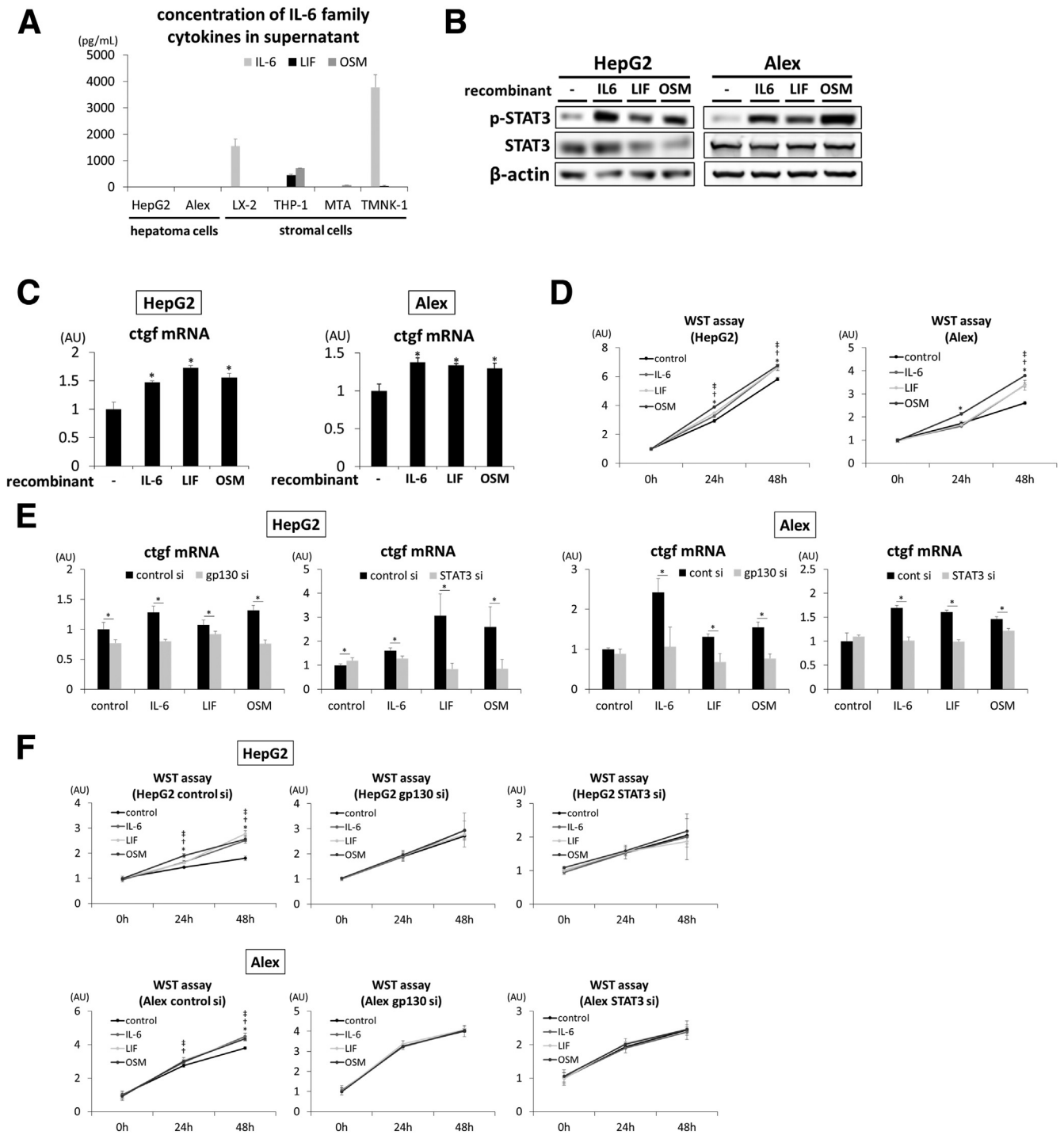
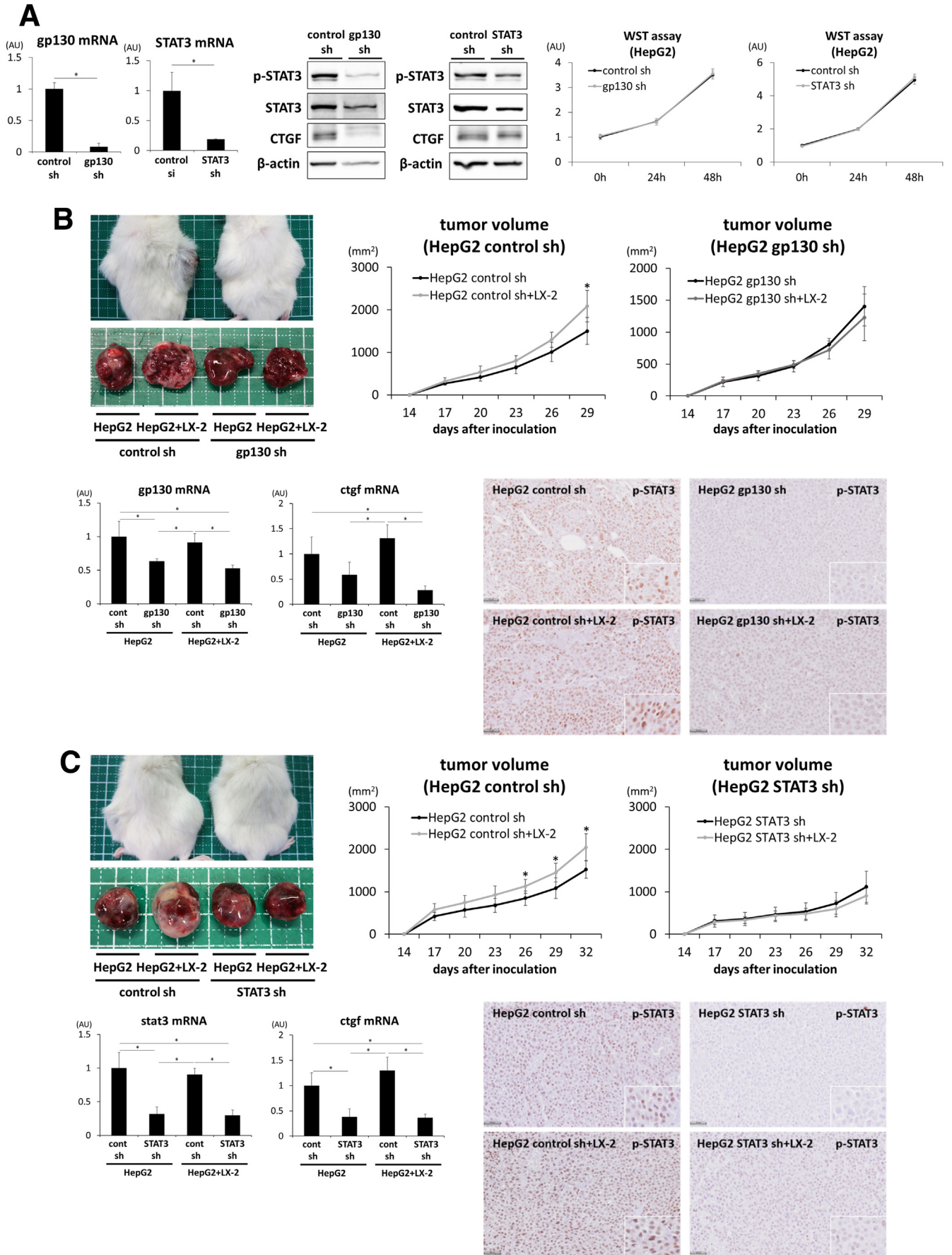


Figure 5. IL-6 family cytokines increased p-STAT3 and CTGF expression in hepatoma cells and enhanced cell proliferation. Concentrations of IL-6, LIF, and OSM in the culture supernatant (A). Culture supernatant was collected 24 hours after the initiation of HepG2, Alex, LX-2, THP-1, MTA, and TMNK-1 cell monoculture. IL-6, LIF, or OSM concentration was measured by enzyme-linked immunosorbent assay. THP-1 cells were pretreated with 100 ng/mL phorbol 12-myristate 13-acetate (PMA) for 48 hours to induce macrophage differentiation, and the culture medium was replaced with PMA-free medium 24 hours before supernatant collection. HepG2 cells and Alex cells were treated with recombinant proteins of IL-6 (20 ng/mL), LIF (1:1000), or OSM (20 ng/mL) (B-D). Cells were serum-starved for 16 hours before the addition of recombinant proteins. B, Protein expression 1 hour after recombinant protein treatment. C, mRNA expression of CTGF 3 hours after recombinant protein treatment. D, WST-8 assay at the indicated time points after treatment with recombinant proteins. HepG2 cells and Alex cells were transfected with gp130 siRNA, STAT3 siRNA, or control siRNA 48 hours before the addition of recombinant proteins (E-F). Recombinant proteins were added 16 hours after serum starvation. E, mRNA expression of CTGF 3 hours after treatment with recombinant proteins. F, WST-8 assay at the indicated time points after recombinant protein treatment (n = 3-4). *P < .05.



experiments. Although cell lines can be easily cultured, their physiological and biochemical characteristics might be altered and may not adequately represent *in vivo* characteristics, because the cells are genetically modified. Primary cells directly isolated from body tissues are more favorable to mimic the *in vivo* state. Recent advancements in organoid culture technology have allowed 3D-coculture of tumor cells and stromal cells, which more precisely replicates tumor microenvironment of HCC.³⁵ In a future study, these novel techniques may hopefully provide a better understanding of CTGF-mediated tumor-stroma cross talk in HCC.

In conclusion, STAT3 and CTGF in hepatoma cells mutually activate each other via IL-6 family cytokine-mediated tumor-stroma cross talk to promote HCC progression. CTGF was shown to be a master regulator of IL-6 family production and STAT3 activation in HCC. Our findings demonstrate a novel cellular and molecular mechanism of STAT3 activation and CTGF overexpression in HCC, and they support the rationale that STAT3 and CTGF, particularly their mutual upregulation mechanism, are therapeutic targets in HCC.

Materials and Methods

Human Samples

Liver samples for immunohistochemistry were collected from patients with HCC who underwent surgical hepatectomy at Osaka University Hospital. This analysis was approved by the Institutional Review Board Committees at Osaka University Hospital (IRB Nos. 13556 and 15267). For scRNA-seq of HCC, we excluded patients who underwent chemotherapy or radiation before hepatectomy and 12 patients undergoing surgical resection for HCC at the National Center for Global Health and Medicine were included.¹⁹ Approval for the use of the resected samples was obtained from the Ethics Committee of the National Center for Global Health and Medicine. Written informed consent was obtained from all the patients included in this study. The experimental protocol conformed to the ethical principles of the Declaration of Helsinki.

Mice

C57BL/6/129 background mice carrying a lox P-stop-lox P (LSL) termination sequence followed by the *Kras*^{G12D} point mutation allele (*Kras*^{LSL-G12D/+}) have been previously described.^{18,36} To generate hepatocyte-specific *Kras*-mutant mice (*Kras*^{LSL-G12D/+}Alb-Cre;*Kras*^{G12D} mice), *Kras*^{LSL-G12D/+} mice were crossed with heterozygous Alb-Cre transgenic mice that expressed the Cre recombinase gene under the

promoter of the albumin gene.¹⁸ C57BL/6 background Mice carrying a STAT3 gene with 2 loxP sequences flanking exon 22 (*STAT3*^{fl/fl}) have been previously described.^{21,22} C57BL/6 background mice that carried 2 floxed CTGF alleles (*CTGF*^{fl/fl}) have been previously described.¹⁸ We generated hepatocyte-specific STAT3-deficient *Kras*-mutant mice by mating *Kras*^{G12D} mice with STAT3-floxed mice. Similarly, *Kras*^{G12D} mice and CTGF-floxed mice were mated to generate hepatocyte-specific CTGF-deficient *Kras*-mutant mice. The littermates were used to compare the phenotypes between experimental groups. NOD/Shi-scid/IL-2R γ (null) (NOG) mice have been previously described.³⁷ Only male mice were used in all the experiments. Mice were maintained under specific pathogen-free conditions and treated with humane care under approval from the Animal Care and Use Committee of Osaka University Medical School.

Cell Culture

The HepG2 and Alex human hepatoma cell lines were obtained from the Japanese Collection of Research Bioresources/Health Science Research Resources Bank (JCRB/HSRRB) cell bank (Osaka, Japan) (JCRB Cat# NIHS0326, RRID:CVCL_0027 and JCRB Cat# JCRB0406, RRID:CVCL_0485, respectively). The LX-2 human HSC line was purchased from Merck Millipore (Darmstadt, Germany) (Millipore Cat# SCC064, RRID:CVCL_5792). THP-1 human monocytes were obtained from American Type Culture Collection (American Type Culture Collection, Manassas, VA) (ATCC Cat# TIB-202, RRID:CVCL_0006). The MTA human T cell line and TMNK-1 liver sinusoidal endothelial cell line were purchased from the JCRB/HSRRB Cell Bank (JCRB Cat# IFO50513, RRID:CVCL_3032 and JCRB Cat# JCRB1564, RRID:CVCL_4W79, respectively). Cells with the passage number of less than 30 were used for all experiments. The HepG2, Alex, LX-2, and TMNK-1 cells were cultured in Dulbecco's modified Eagle's medium (Sigma-Aldrich, St. Louis, MO) at 37 °C with 5% CO₂, and THP-1 and MTA cells were cultured in RPMI-1640. The media was supplemented with 10% fetal calf serum and antibiotics unless otherwise indicated. A Transwell insert system (Corning, Corning, NY) was used for coculture experiments. To induce differentiation into macrophages, THP-1 cells were treated with 100 ng/mL phorbol 12-myristate 13-acetate (Sigma-Aldrich) for 48 hours. A WST-8 assay (Nacalai Tesque, Kyoto, Japan) was performed to analyze cell proliferation. Recombinant human IL-6, LIF, and OSM proteins were purchased from Thermo Fisher Scientific (Waltham, MA), FUJIFILM Wako Pure Chemical Corporation (Osaka, Japan), R&D Systems (Minneapolis, MN), and R&D Systems, respectively. Recombinant

Figure 6. (See previous page). Inhibition of gp130/STAT3 signaling abolished the accelerated growth of HepG2 cells injected with LX-2 cells and downregulated CTGF expression in xenograft tumors. Protein and mRNA expression and proliferation in HepG2 cells stably expressing STAT3, gp130, or control shRNA *in vitro* (A). RNA and proteins were extracted 24 hours after plating. WST-8 assay was performed to evaluate cell proliferation at indicated time points. Xenograft models of HepG2 cells stably expressing STAT3, gp130, or control shRNA with or without LX-2 cells (B-C). HepG2 cells stably expressing gp130 shRNA (B), STAT3 shRNA (C), or control shRNA were subcutaneously injected alone or with the same number of LX-2 cells into the left and right flank portions of NOG mice, respectively. Representative images of xenograft tumors, tumor volume measured sequentially, mRNA expression, and immunohistochemistry for p-STAT3 (scale bar: 50 μ m) in xenograft tumors are presented (n = 4-5). **P* < .05 vs control.

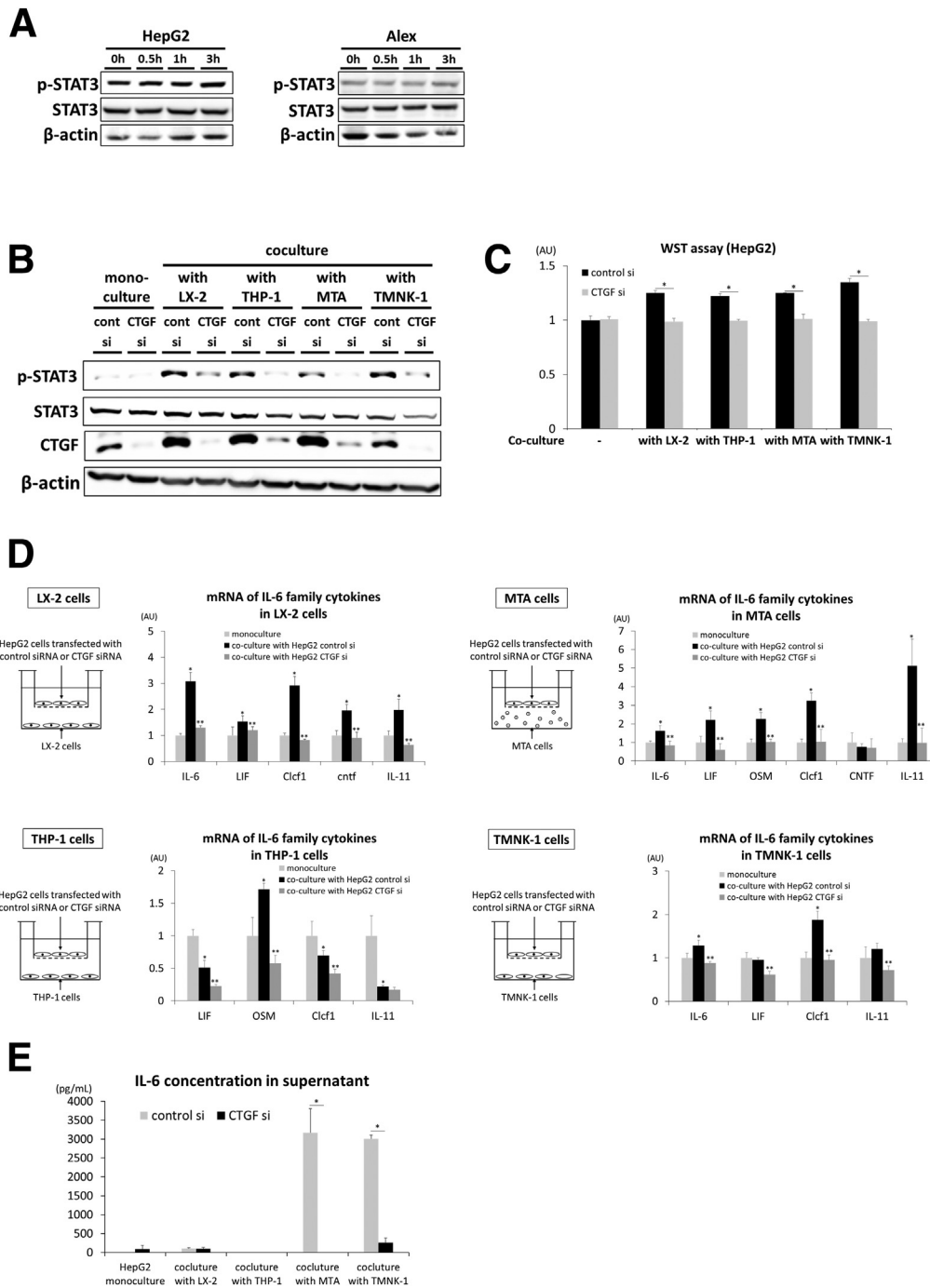


Figure 7. Knockdown of CTGF in HepG2 cells decreased IL-6 family cytokine expression in stromal cells, down-regulated p-STAT3 expression in HepG2 cells and reduced the proliferation of HepG2 cells. Western blotting of HepG2 or Alex cells treated with recombinant CTGF protein under monoculture (A). Protein lysate was collected from cells 0, 0.5, 1, and 3 hours after the addition of 5 nM recombinant CTGF protein. HepG2 cells were incubated under monoculture or coculture with stromal cell lines (B-E). HepG2 cells were transfected with CTGF siRNA or control siRNA 48 hours before coculturing. Total proteins and RNA were collected after 24 hours of coculture. THP-1 cells had been pretreated with 100 ng/ml phorbol 12-myristate 13-acetate (PMA) for 48 hours to induce macrophage differentiation before coculture. B, Western blot showing HepG2 cell proteins in monoculture or cocultured with LX-2, THP-1, MTA, and TMNK-1 cells. C, WST-8 assay of HepG2 cells performed 48 hours after initiation of monoculture or coculture (n = 3). *P < .05. D, mRNA expression of IL-6 family cytokines in stromal cell lines in monoculture or cocultured with HepG2 cells transfected with CTGF siRNA or control siRNA (n = 4). E, IL-6 concentration in supernatant measured via enzyme-linked immunosorbent assay (n = 4). *P < .05 vs monoculture; **P < .05 vs coculture with HepG2 control si.

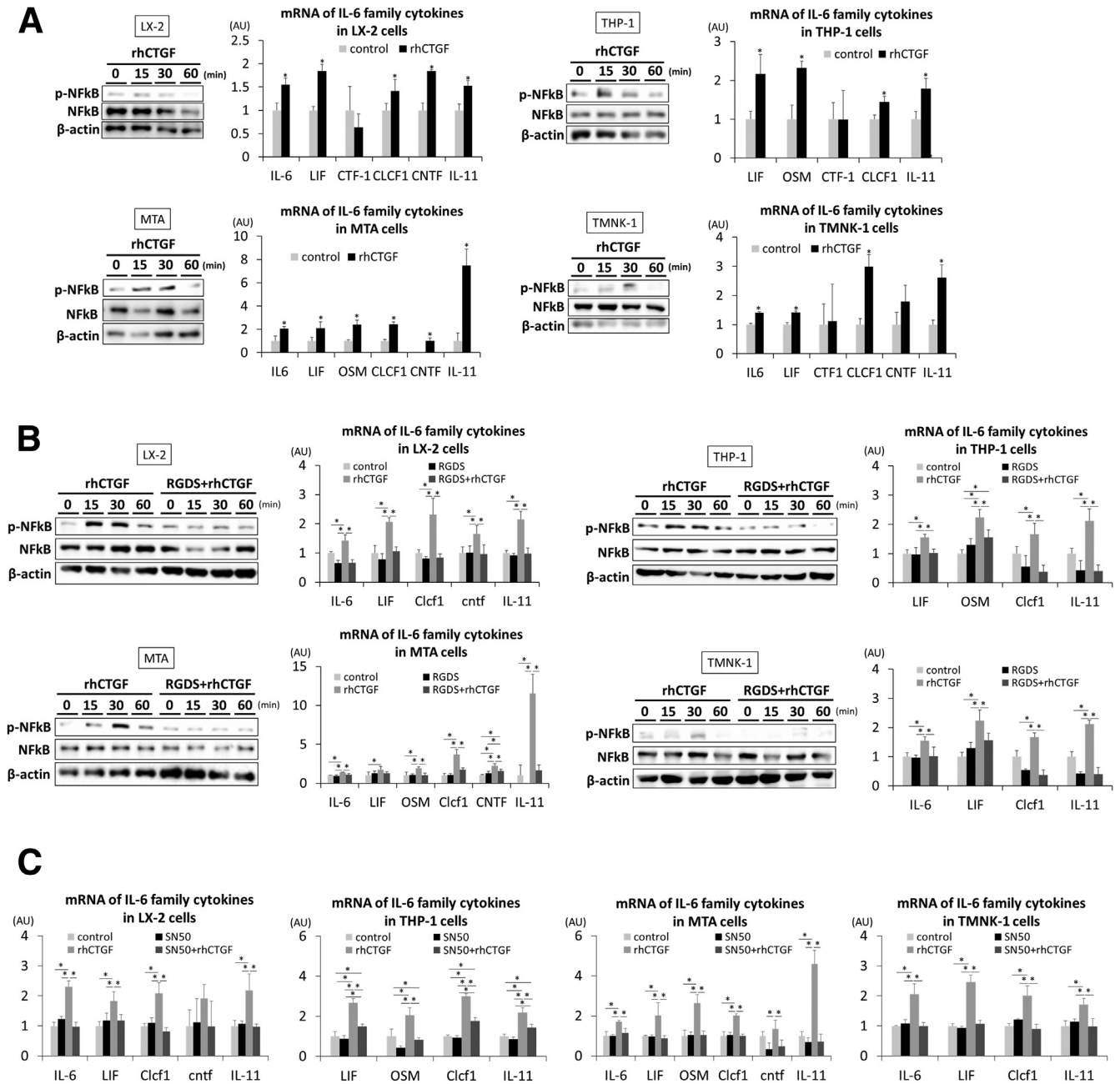


Figure 8. Recombinant CTGF treatment upregulated IL-6 family cytokine expression in stromal cell lines via integrin/NF- κ B signaling. LX-2, THP-1, MTA, and TMNK-1 cells were serum-starved for 16 hours and then treated with 5 nM recombinant CTGF protein. THP-1 cells had been pretreated with 100 ng/mL phorbol 12-myristate 13-acetate (PMA) to induce macrophage differentiation for 48 hours before starvation. Total protein was collected at the indicated time points after the addition of recombinant CTGF protein. Total RNA was extracted 6 hours after incubation with recombinant CTGF protein. Protein and gene expression after recombinant CTGF treatment (A-C). Cells were treated with recombinant CTGF alone (A) or pretreated with 1 mM RGDS peptide (B) or 50 ng/mL SN-50 (C) for 2 hours before the addition of recombinant CTGF protein. n = 4 (A, B) or n = 3 (C). *P < .05.

CTGF protein was kindly provided by FibroGen (San Francisco, CA). SN-50 (FUJIFILM Wako Pure Chemical Corporation) was used as an NF- κ B inhibitor. The pan-integrin inhibitor RGDS peptide was purchased from R&D Systems. siRNA against STAT3, gp130, and CTGF and control siRNA were purchased from Thermo Fisher Scientific and

transfected into the cells using Lipofectamine RNAiMAX (Thermo Fisher Scientific) according to the Lipofectamine reverse transfection protocol. A STAT3 shRNA plasmid (Santa Cruz Biotechnology, Dallas, TX), gp130 shRNA plasmid (Santa Cruz Biotechnology) or control shRNA plasmid (Santa Cruz Biotechnology) was transfected

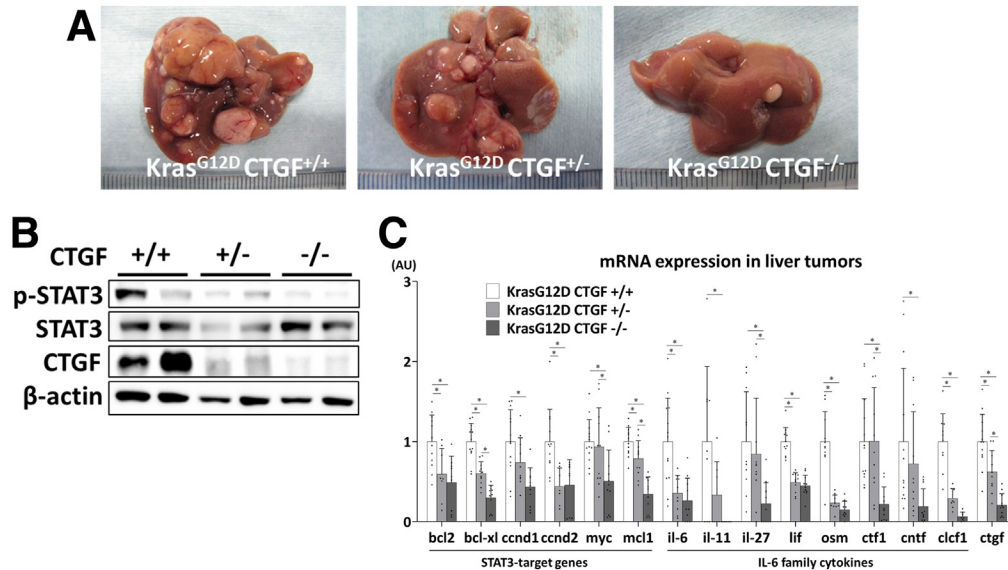


Figure 9. Hepatocyte-specific knockout of CTGF downregulated IL-6 family cytokine expression in liver tumors of $Kras^{G12D}$ mice and suppressed STAT3 activation and tumor progression. By mating $Kras^{G12D}$ mice with CTGF-floxed mice, we generated hepatocyte-specific CTGF-knockout $Kras^{G12D}$ mice. After crossing CTGF^{fl/+} $Kras^{G12D}$ mice and CTGF^{fl/+} $Kras^{LSL-G12D/+}$ mice, the following littermates were obtained: (1) $Kras^{G12D}$ CTGF^{+/+} (CTGF^{fl/+} $Kras^{LSL-G12D/+}$ Alb-Cre); (2) $Kras^{G12D}$ CTGF^{+/-} (CTGF^{fl/+} $Kras^{LSL-G12D/+}$ Alb-Cre); and (3) $Kras^{G12D}$ CTGF^{-/-} (CTGF^{fl/fl} $Kras^{LSL-G12D/+}$ Alb-Cre). The phenotypes were evaluated at 8 months of age. A, Representative images of 8-month-old mice. B, Western blot showing liver tumor proteins. C, mRNA expression of CTGF, STAT3 target genes, and IL-6 family cytokines in liver tumors (n = 7-13). * $P < .05$.

according to the manufacturer's protocol. Stably transfected cells were selected through puromycin (Thermo Fisher Scientific) treatment. Several single colonies were isolated through selection.

Experimental Protocol for Xenograft Tumor Models

Detailed procedure was described previously.¹⁸ Briefly, hepatoma cells with or without the same number of LX-2 cells suspended in Matrigel (Corning) were subcutaneously inoculated into NOG mice. The length and width of the subcutaneous tumors were measured twice per week. Tumor volume was calculated as previously reported.¹⁸

DEN-induced Liver Carcinogenesis Model

DEN (Sigma-Aldrich) (20 mg/kg) was intraperitoneally injected into 2-week-old male mice to chemically induce liver carcinogenesis.

Enzyme-linked Immunosorbent Assay

To measure the concentration in the cell culture supernatant, commercial enzyme-linked immunosorbent assay kits for IL-6 (PeproTech, Rocky Hill, NJ), LIF (R&D Systems), and OSM (R&D Systems) were used according to the manufacturer's recommended protocols.

Histological Analyses

Liver sections were routinely formalin-fixed and paraffin-embedded and stained with HE. Immunohistochemistry was

performed using paraffin-embedded liver sections subjected to antibodies listed in Table 3. The number of PCNA-positive cells was counted in high-power fields at 400-fold magnification.

RNA Isolation and qRT-PCR

Total cell or tissue RNA was extracted with a RNeasy Mini Kit (QIAGEN, Hilden, Germany) according to the manufacturer's recommended protocols. cDNA was subsequently produced by reverse transcription.¹⁸ Gene expression was measured by real-time RT-PCR using TaqMan Gene Expression Assays (Thermo Fisher Scientific) as follows: mouse-ctgf (Mm01192933_g1), mouse-bcl-2 (Mm00477631_m1), mouse-bcl-xl (Mm00437783_m1), mouse-cyclin d1 (Mm00432359_m1), mouse-cyclin d2 (Mm00438070_m1), mouse-myc (Mm00487804_m1), mouse-il-6 (Mm00446190_m1), mouse-lif (Mm00434762_g1), mouse-osm (Mm01193966_m1), mouse-il-11 (Mm00434162_m1), mouse-il-22 (Mm01226722_g1), mouse-il-27 (Mm00461163_g1), mouse-il-31 (Mm01194496_m1), mouse-ctf1 (Mm00432772_m1), mouse-cntf (Mm00446373_m1), mouse-clcf1 (Mm01236492_m1), mouse- β -actin (Mm02619580_g1), human-ctgf (Hs00170014_m1), human-il-6 (Hs00174131_m1), human-lif (Hs01055668_m1), human-osm (Hs00171165_m1), human-il-11 (Hs01055413_g1), human-il-22 (Hs01574154_m1), human-il-27 (Hs00377366_m1), human-il-31 (Hs01098710_m1), human-ctf1 (Hs00173498_m1), human-cntf (Hs00173456_m1), human-clcf1 (Hs00757942_m1), human-stat3 (Hs00374280_m1), human-gp130 (Hs00174360_m1), and human- β -actin (Hs01060665_g1). The expression level of each gene was normalized to that of β -actin.

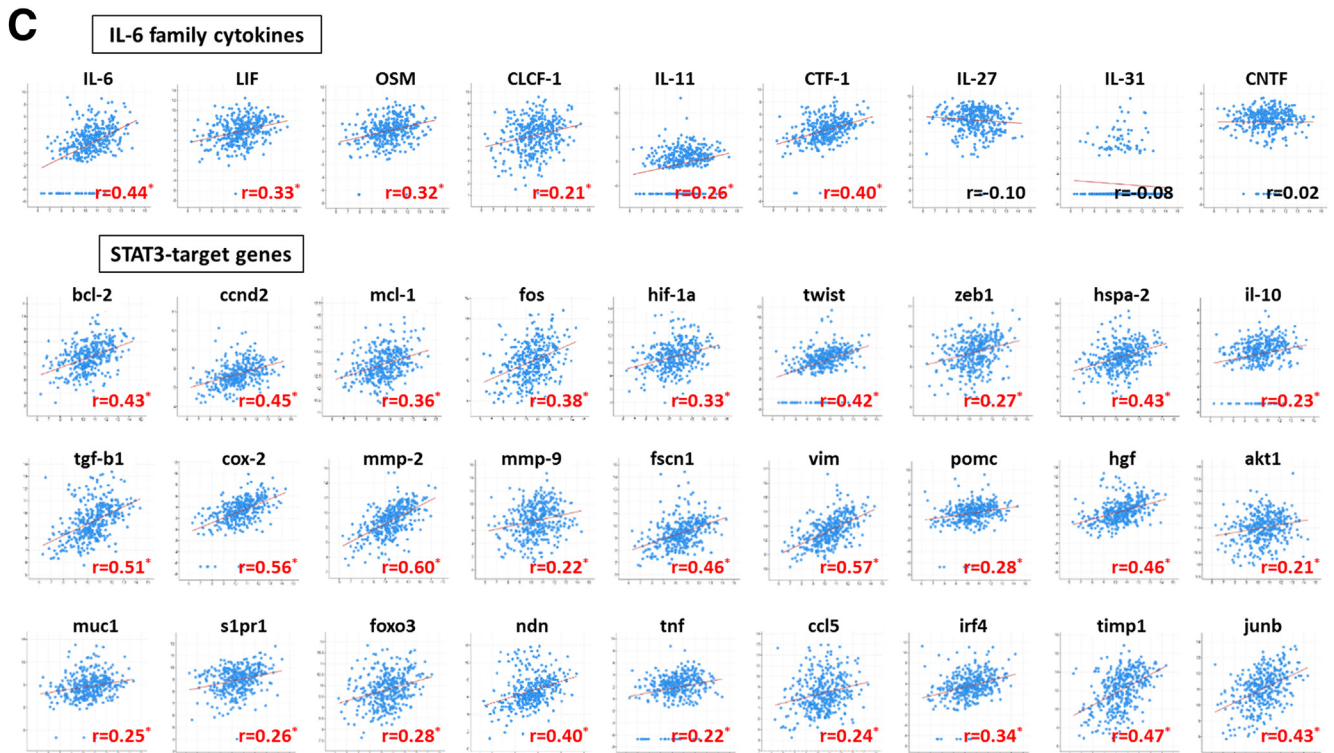
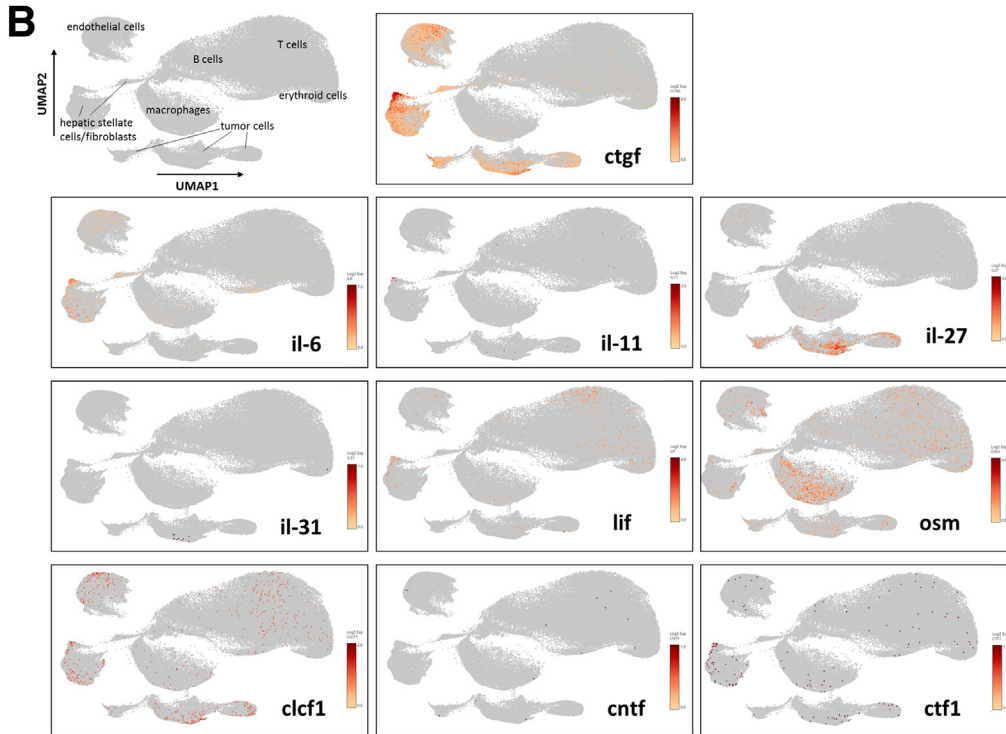
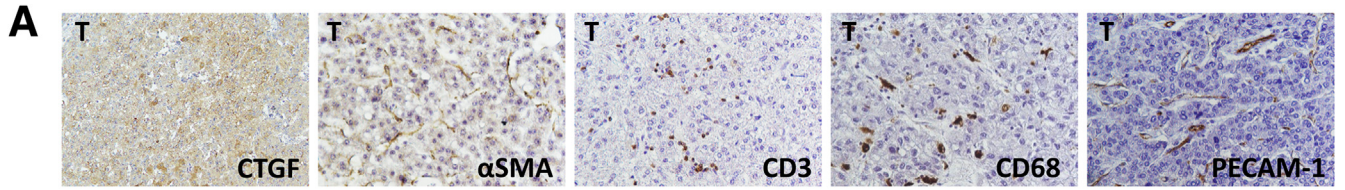


Table 3. Antibodies Used for This Study

Target	Source	Identifier
CTGF	Santa Cruz Biotechnology	Cat# sc-14939, RRID:AB 638805
α -SMA	Abcam	Cat# ab5694, RRID:AB 2223021
F4/80	Bio-Rad	Cat# MCA497RT, RRID:AB 1102558
CD68	Abcam	Cat# ab955, RRID:AB 307338
CD3	Abcam	Cat# ab11089, RRID:AB 2889189
PECAM1	Abcam	Cat# ab28364, RRID:AB 726362
PCNA	Cell Signaling Technology	Cat# 2586, RRID:AB 2160343
p-STAT3 (for Western blotting)	Cell Signaling Technology	Cat# 9145, RRID:AB 2491009
p-STAT3 (for immunohistochemistry)	Abcepta, Inc.	Cat# AP3261A-EV
STAT3	Cell Signaling Technology	Cat# 4904, RRID:AB 331269
p-Smad3	Cell Signaling Technology	Cat# 9520, RRID:AB 2193207
p-Smad2	Cell Signaling Technology	Cat# 18338, RRID:AB 2798798
p-Erk	Cell Signaling Technology	Cat#9101, RRID:AB 331646
p-Akt	Cell Signaling Technology	Cat# 9271, RRID:AB 329825
p-NF- κ B	Cell Signaling Technology	Cat# 3033, RRID:AB 331284
NF- κ B	Cell Signaling Technology	Cat# 8242, RRID:AB 10859369
β -actin	Sigma-Aldrich	Cat# A5316, RRID:AB 476743

α -SMA, Alpha smooth muscle actin; CTGF, connective tissue growth factor; NF- κ B, nuclear factor kappa B; PECAM-1, platelet endothelial cell adhesion molecule-1; STAT3, signal transducer and activator of transcription 3.

Western Blot Analysis

To extract proteins from liver tissues, samples were lysed in lysis buffer (1% Nonidet P-40, 0.5% sodium deoxycholate, 0.1% sodium dodecyl sulfate, protease inhibitor cocktail [Nacalai Tesque], phosphatase inhibitor cocktail [Nacalai Tesque], and phosphate buffered saline, pH 7.4). Electrophoresis was performed to separate proteins in sodium dodecyl sulfate polyacrylamide gels. The samples were subsequently transferred onto a polyvinylidene fluoride membrane. Antibodies listed in Table 3 were used for immunodetection.

scRNA-seq and Data Analysis

Protocols for scRNA-seq and data analysis of human HCC were described previously.¹⁹ Briefly, surgically resected HCC samples were cut into pieces and enzymatically digested into single-cell suspensions. scRNA-seq libraries were prepared using a Chromium Single Cell 3' Library Construction Kit (10X Genomics, Pleasanton, CA). The libraries were sequenced on an Illumina HiSeq 2500 system and a Nova-seq sequencer (Illumina, San Diego, CA). Data analyses were performed according to the Cell Ranger protocol (10X Genomics) to determine the number of gene transcripts per cell. The results were visualized using Loupe Cell Browser, version 3.1 (10X Genomics) (Loupe Browser, RRID:SCR_018555). Murine liver tumor tissues were

enucleated from the liver and enzymatically dissociated into a single-cell suspension using a tumor dissociation kit (Miltenyi Biotec, Bergisch Gladbach, Germany). The single-cell suspension was then loaded into a BD Rhapsody cartridge (BD Biosciences, San Jose, CA) to isolate the single-cell transcriptome. scRNA-seq libraries were generated using a BD Rhapsody WTA amplification kit (BD Biosciences). The libraries were sequenced by a DNBSEQ-G400RS (MGI Tech, China) platform in 2×100 bp paired-end mode. BD Rhapsody WTA Analysis Pipeline on Seven Bridges Genomics (<https://www.sevenbridges.com/>) was used for alignment, filtering, and unique molecular identifier counting to determine the number of mRNA molecules per cell. GRCm38 was used as a reference for genome assembly and annotation. SeqGeq software (BD Biosciences) was used for concatenation of the outputs from multiple independent samples, and then, normalization, quality control, batch correction, dimensionality reduction, and clustering were performed to visualize the results. Processed data, as well as raw data, was deposited in Gene Expression Omnibus (GEO) database (GSE192697).

Analysis of Public Clinical Datasets

We obtained RNA-seq data of 373 HCC samples obtained from The Cancer Genome Atlas (<https://portal.gdc.cancer.gov/projects/TCGA-LIHC>). Data analysis was performed

Figure 10. (See previous page). CTGF expression was positively correlated with that of STAT3 target genes and IL-6 family cytokines which were mainly expressed in stromal cells in human HCC. Immunohistochemical staining for CTGF, α SMA, CD3, CD68, and PECAM-1 in human HCC (200 \times) A,. A representative image of each molecule from 6 samples is presented. Samples taken from surgically resected HCC tissues were subjected to scRNA-seq (n = 12) (B-C). B, UMAP showing CTGF and IL-6 family cytokines. Correlation of mRNA expression between CTGF and STAT3-target genes or IL-6 family cytokines in 373 HCC samples obtained from the The Cancer Genome Atlas database (C). Correlation coefficients presented in red were statistically significant. * $P < .05$.

with the cBioPortal for Cancer Genomics website (<http://cbioportal.org>).

The DNA sequence of the enhancer in the human ctgf gene is available at the VISTA Enhancer Browser (http://enhancer.lbl.gov/cgi-bin/imagenb3.pl?form=presentation&show=1&experiment_id=2544&organism_id=1) (VISTA Enhancer Browser, RRID:SCR_007973). The STAT3-binding site in this enhancer sequence of the human ctgf gene was found with the UCSC Genome Browser (http://genome.ucsc.edu/cgi-bin/hgTracks?db=hg19&lastVirtModeType=default&lastVirtModeExtraState=&virtModeType=default&virtMode=0&nonVirtPosition=&position=chr6%3A132274880%2D132277674&hgid=1156684129_AbHGda4GRGJWYAhET6sdtTEZa6b) (UCSC Genome Browser, RRID:SCR_005780).

Statistical Analysis

Differences between unpaired groups with normal distributions were compared using the Student *t* test. Correlations were assessed using the Spearman rank correlation coefficient. The χ^2 test was performed to analyze categorical data. Parametric multiple comparisons were performed by 1-way analysis of variance followed by Tukey-Kramer post hoc test. *P*-values of less than .05 were considered to indicate statistical significance.

References

- Zhong Z, Wen Z, Darnell JE Jr. Stat3: a STAT family member activated by tyrosine phosphorylation in response to epidermal growth factor and interleukin-6. *Science* 1994;264:95–98.
- Huynh J, Chand A, Gough D, Ernst M. Therapeutically exploiting STAT3 activity in cancer - using tissue repair as a road map. *Nat Rev Cancer* 2019;19:82–96.
- Bromberg JF, Wrzeszczynska MH, Devgan G, Zhao Y, Pestell RG, Albanese C, Darnell JE Jr. Stat3 as an oncogene. *Cell* 1999;98:295–303.
- Carpenter RL, Lo HW. STAT3 target genes relevant to human cancers. *Cancers (Basel)* 2014;6:897–925.
- Yang JD, Hainaut P, Gores GJ, Amadou A, Plymoth A, Roberts LR. A global view of hepatocellular carcinoma: trends, risk, prevention and management. *Nat Rev Gastroenterol Hepatol* 2019;16:589–604.
- Llovet JM, Kelley RK, Villanueva A, Singal AG, Pikarsky E, Roayaie S, Lencioni R, Koike K, Zucman-Rossi J, Finn RS. Hepatocellular carcinoma. *Nat Rev Dis Primers* 2021;7:6.
- Simard EP, Ward EM, Siegel R, Jemal A. Cancers with increasing incidence trends in the United States: 1999 through 2008. *CA Cancer J Clin* 2012;62:118–128.
- He G, Karin M. NF-kappaB and STAT3 - key players in liver inflammation and cancer. *Cell Res* 2011;21:159–168.
- Calvisi DF, Ladu S, Gorden A, Farina M, Conner EA, Lee JS, Factor VM, Thorgeirsson SS. Ubiquitous activation of Ras and Jak/Stat pathways in human HCC. *Gastroenterology* 2006;130:1117–1128.
- Li WC, Ye SL, Sun RX, Liu YK, Tang ZY, Kim Y, Karras JG, Zhang H. Inhibition of growth and metastasis of human hepatocellular carcinoma by antisense oligonucleotide targeting signal transducer and activator of transcription 3. *Clin Cancer Res* 2006;12:7140–7148.
- He G, Yu GY, Temkin V, Ogata H, Kuntzen C, Sakurai T, Sieghart W, Peck-Radosavljevic M, Leffert HL, Karin M. Hepatocyte IKKbeta/NF-kappaB inhibits tumor promotion and progression by preventing oxidative stress-driven STAT3 activation. *Cancer Cell* 2010;17:286–297.
- Bard-Chapeau EA, Li S, Ding J, Zhang SS, Zhu HH, Princen F, Fang DD, Han T, Bailly-Maitre B, Poli V, Varki NM, Wang H, Feng GS. Ptpn11/Shp2 acts as a tumor suppressor in hepatocellular carcinogenesis. *Cancer Cell* 2011 17;19:629–639.
- Wang H, Lafdil F, Wang L, Park O, Yin S, Niu J, Miller AM, Sun Z, Gao B. Hepatoprotective versus oncogenic functions of STAT3 in liver tumorigenesis. *Am J Pathol* 2011;179:714–724.
- Abe M, Yoshida T, Akiba J, Ikezono Y, Wada F, Masuda A, Sakaue T, Tanaka T, Iwamoto H, Nakamura T, Sata M, Koga H, Yoshimura A, Torimura T. STAT3 deficiency prevents hepatocarcinogenesis and promotes biliary proliferation in thioacetamide-induced liver injury. *World J Gastroenterol* 2017;23:6833–6844.
- Calvisi DF. Dr. Jekyll and Mr. Hyde: a paradoxical oncogenic and tumor suppressive role of signal transducer and activator of transcription 3 in liver cancer. *Hepatology* 2011;54:9–12.
- Feng GS. Conflicting roles of molecules in hepatocarcinogenesis: paradigm or paradox. *Cancer Cell* 2012;21:150–154.
- Lee C, Cheung ST. STAT3: an emerging therapeutic target for hepatocellular carcinoma. *Cancers (Basel)* 2019;11:1646.
- Makino Y, Hikita H, Kodama T, Shigekawa M, Yamada R, Sakamori R, Eguchi H, Morii E, Yokoi H, Mukoyama M, Hiroshi S, Tatsumi T, Takehara T. CTGF mediates tumor-stroma interactions between hepatoma cells and hepatic stellate cells to accelerate HCC progression. *Cancer Res* 2018;78:4902–4914.
- Myojin Y, Hikita H, Sugiyama M, Sasaki Y, Fukumoto K, Sakane S, Makino Y, Takemura N, Yamada R, Shigekawa M, Kodama T, Sakamori R, Kobayashi S, Tatsumi T, Suemizu H, Eguchi H, Kokudo N, Mizokami M, Takehara T. Hepatic stellate cells in hepatocellular carcinoma promote tumor growth via growth differentiation factor 15 production. *Gastroenterology* 2021;160:1741–1754.e16.
- Geng ZM, Li QH, Li WZ, Zheng JB, Shah V. Activated human hepatic stellate cells promote growth of human hepatocellular carcinoma in a subcutaneous xenograft nude mouse model. *Cell Biochem Biophys* 2014;70:337–347.
- Sakamori R, Takehara T, Ohnishi C, Tatsumi T, Ohkawa K, Takeda K, Akira S, Hayashi N. Signal transducer and activator of transcription 3 signaling within hepatocytes attenuates systemic inflammatory response and lethality in septic mice. *Hepatology* 2007;46:1564–1573.
- Sakamori R, Takehara T, Tatsumi T, Shigekawa M, Hikita H, Hiramatsu N, Kanto T, Hayashi N. STAT3 signaling within hepatocytes is required for anemia of inflammation in vivo. *J Gastroenterol* 2010;45:244–248.

23. Lokau J, Schoeder V, Haybaeck J, Garbers C. Jak-stat signaling induced by interleukin-6 family cytokines in hepatocellular carcinoma. *Cancers (Basel)* 2019; 11:1704.
24. Jones SA, Jenkins BJ. Recent insights into targeting the IL-6 cytokine family in inflammatory diseases and cancer. *Nat Rev Immunol* 2018;18:773–789.
25. Naugler WE, Sakurai T, Kim S, Maeda S, Kim K, Elsharkawy AM, Karin M. Gender disparity in liver cancer due to sex differences in MyD88-dependent IL-6 production. *Science* 2007;317:121–124.
26. Wang X, Hassan W, Jabeen Q, Khan GJ, Iqbal F. Interdependent and independent multidimensional role of tumor microenvironment on hepatocellular carcinoma. *Cytokine* 2018;103:150–159.
27. Hernandez-Gea V, Toffanin S, Friedman SL, Llovet JM. Role of the microenvironment in the pathogenesis and treatment of hepatocellular carcinoma. *Gastroenterology* 2013;144:512–527.
28. Yang JD, Nakamura I, Roberts LR. The tumor microenvironment in hepatocellular carcinoma: current status and therapeutic targets. *Semin Cancer Biol* 2011; 21:35–43.
29. Jun JI, Lau LF. Taking aim at the extracellular matrix: CCN proteins as emerging therapeutic targets. *Nat Rev Drug Discov* 2011;10:945–963.
30. Shen YW, Zhou YD, Chen HZ, Luan X, Zhang WD. Targeting CTGF in cancer: an emerging therapeutic opportunity. *Trends Cancer* 2021;7:511–524.
31. Neesse A, Frese KK, Bapiro TE, Nakagawa T, Sternlicht MD, Seeley TW, Pilarsky C, Jodrell DI, Spong SM, Tuveson DA. CTGF antagonism with mAb FG-3019 enhances chemotherapy response without increasing drug delivery in murine ductal pancreas cancer. *Proc Natl Acad Sci U S A* 2013;110: 12325–12330.
32. Picozzi V, Alseidi A, Winter J, Pishvaian M, Mody K, Glaspy J, Larson T, Matrana M, Carney M, Porter S, Kouchakji E, Rocha F, Carrier E. Gemcitabine/nab-paclitaxel with pamrevlumab: a novel drug combination and trial design for the treatment of locally advanced pancreatic cancer. *ESMO Open* 2020;5:e000668.
33. Chen J, Zaidi S, Rao S, Chen JS, Phan L, Farci P, Su X, Shetty K, White J, Zamboni F, Wu X, Rashid A, Pattabiraman N, Mazumder R, Horvath A, Wu RC, Li S, Xiao C, Deng CX, Wheeler DA, Mishra B, Akbani R, Mishra L. Analysis of genomes and transcriptomes of hepatocellular carcinomas identifies mutations and gene expression changes in the transforming growth factor- β pathway. *Gastroenterology* 2018;154:195–210.
34. Ito Y, Sasaki Y, Horimoto M, Wada S, Tanaka Y, Kasahara A, Ueki T, Hirano T, Yamamoto H, Fujimoto J, Okamoto E, Hayashi N, Hori M. Activation of mitogen-activated protein kinases/extracellular signal-regulated kinases in human hepatocellular carcinoma. *Hepatology* 1998;27:951–958.
35. Liu J, Li P, Wang L, Li M, Ge Z, Noordam L, Lieshout R, Versteegen MMA, Ma B, Su J, Yang Q, Zhang R, Zhou G, Carrascosa LC, Sprengers D, IJzermans JNM, Smits R, Kwekkeboom J, van der Laan LJW, Peppelenbosch MP, Pan Q, Cao W. Cancer-associated fibroblasts provide a stromal niche for liver cancer organoids that confers trophic effects and therapy resistance. *Cell Mol Gastroenterol Hepatol* 2021;11:407–431.
36. Makino Y, Hikita H, Fukumoto K, Sung JH, Sakano Y, Murai K, Sakane S, Kodama T, Sakamori R, Kondo J, Kobayashi S, Tatsumi T, Takehara T. Constitutive activation of the tumor suppressor p53 in hepatocytes paradoxically promotes non-cell autonomous liver carcinogenesis. *Cancer Res* 2022;82:2860–2873.
37. Ito M, Hiramatsu H, Kobayashi K, Suzue K, Kawahata M, Hioki K, Ueyama Y, Koyanagi Y, Sugamura K, Tsuji K, Heike T, Nakahata T. NOD/SCID/gamma (c) (null) mouse: an excellent recipient mouse model for engraftment of human cells. *Blood* 2002;100:3175–3182.

Received December 31, 2021. Accepted September 13, 2022.

Correspondence

Address correspondence to: Tetsuo Takehara, MD, PhD, Department of Gastroenterology and Hepatology, Osaka University Graduate School of Medicine, 2-2 Yamadaoka, Suita, Osaka, 565-0871, Japan. e-mail: takehara@gh.med.osaka-u.ac.jp.

Acknowledgment

The authors thank Dr. Hiroshi Suemizu (Department of Laboratory Animal Research, Central Institute for Experimental Animals, Kanagawa, Japan) for offering NOG mice. The authors thank FibroGen for kindly providing a recombinant CTGF protein. The authors also thank Miyuki Imai (Department of Gastroenterology and Hepatology, Osaka University Graduate School of Medicine, Osaka, Japan) for technical support. We acknowledge the NGS core facility of the Genome Information Research Center at the Research Institute for Microbial Diseases of Osaka University for support with scRNA-seq and data analysis.

CRedit Authorship Contributions

Yuki Makino (Data curation: Lead; Funding acquisition: Supporting; Investigation: Lead; Project administration: Equal; Software: Lead; Writing – original draft: Lead)

Hayato Hikita (Conceptualization: Supporting; Funding acquisition: Supporting; Project administration: Equal; Validation: Lead; Writing – original draft: Supporting; Writing review & editing: Supporting)

Seiya Kato (Data curation: Supporting; Investigation: Supporting; Software: Supporting; Validation: Supporting)

Masaya Sugiyama (Data curation: Supporting; Funding acquisition: Supporting; Software: Equal; Visualization: Equal)

Minoru Shigekawa (Data curation: Supporting; Investigation: Supporting)

Tatsuya Sakamoto (Investigation: Supporting)

Yoichi Sasaki (Investigation: Supporting)

Kazuhiro Murai (Investigation: Supporting)

Sadatsugu Sakane (Investigation: Supporting)

Takahiro Kodama (Validation: Supporting)

Ryotaro Sakamori (Validation: Supporting)

Shogo Kobayashi (Resources: Supporting)

Hidetoshi Eguchi (Resources: Supporting)

Nobuyuki Takemura (Data curation: Supporting)

Norihiro Kokudo (Data curation: Supporting; Resources: Supporting)

Hideki Yokoi (Resources: Supporting)

Masashi Mukoyama (Resources: Supporting)

Tomohide Tatsumi (Validation: Supporting)

Tetsuo Takehara, MD, PhD (Conceptualization: Lead; Funding acquisition: Lead; Resources: Lead; Supervision: Lead; Writing – review & editing: Lead)

Conflicts of interest

The authors disclose no conflicts.

Funding

This work was partially supported by a Grant-in-Aid for Early Career Scientists (to Yuki Makino, JP 19K17432), a Grant-in-Aid for Scientific Research (C) (to Hayato Hikita, 20K08307, and to Yuki Makino, 21K08005), a Grant-in-Aid for Scientific Research (B) (to Tetsuo Takehara, JP21H02903) from the Ministry of Education, Culture, Sports, Science, and Technology, Japan, and Grants-in-Aid for Research Programs on Hepatitis from the Japan Agency for Medical Research and Development (to Tetsuo Takehara, JP20fk0210064, to Hayato Hikita, JP22fk0210104, and to Masaya Sugiyama, JP21fk0310111 and JP21fk0310104)